

Plasma Pyrolysis & Incineration
for Nuclear Wastes 6

[¹⁸F] FLT Precursors for
PET Imaging 11

Eco-friendly Biopesticide
Formulation 19



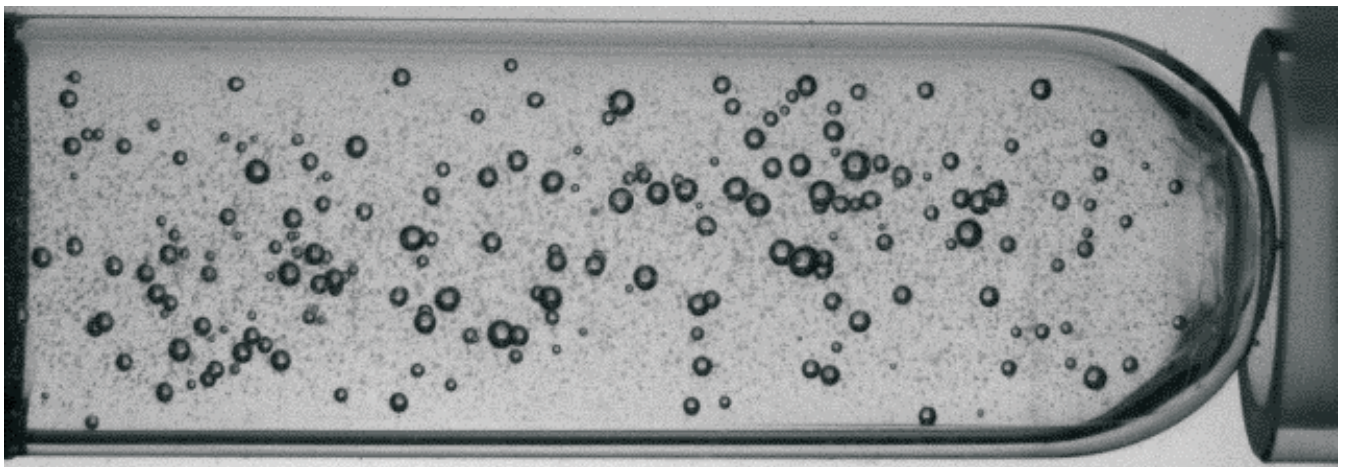
Bi-monthly • November - December • 2020

• Issue No. 370

ISSN: 0976-2108

BARC

NEWSLETTER



**Neutron generated bubbles seen
through detector reader**

BARC Technology
Incubation Centre

Shanti Swarup Bhatnagar
Prize for BARC Scientist

Radio Frequency Power
Amplifiers for FermiLab

This page is intentionally left blank

CONTENTS

Editorial Committee

Chairman

Dr. A.P. Tiwari
KMG

Editor

Dr. G. Ravi Kumar
SIRD

Members

Dr. A.K. Nayak, RED
Dr. G. Sugilal, PSDD
Dr. V.H. Patankar, ED
Dr. (Smt.) B.K. Sapra, RP&AD
Dr. L.M. Pant, NPD
Dr. Ranjan Mittal, SSPD
Dr. (Smt.) S. Mukhopadhyay, ChED
Dr. K.P. Muthe, TPD
Dr. V. Sudarsan, ChD
Dr. A.V.S.S.N. Rao, MBD
Dr. S.R. Shimjith, RCnD
Dr. Sandip Basu, RMC
Dr. Pranesh Sengupta, MSD
Dr. R. Tripathi, RCD

Member Secretary

Shri Madhav N, SIRD

Issue Designed by

Shri Dinesh J. Vaidya, SIRD

1

Titanium Hydride targets for Portable Neutron Generator applications

Mayank Shukla, Niranjana Ramgir, Prashant Singh, Yogesh Kashyap, A.K. Debnath, K.P. Muthe, Tushar Roy, Baribaddala Ravi, Shefali Shukla, S.G. Sawant, S.K. Raut, Ram Avtar Jat, S.C. Parida, K.G. Bhushan and K.C. Rao

6

Plasma Pyrolysis and Incineration for Low Level Radioactive Solid Wastes

K.C.Pancholi, C.P. Kaushik, Suprabha, S. Agarwal, S.K. Solankar, S.K. Mishra, N.S. Tomar, S. Bhandari, S. Ghorui, R.L. Bhardwaj, E. Kandaswamy, M. Martin and A. Sharma

11

Affordable [¹⁸F] FLT Precursors for PET Imaging

K.S. Ajish Kumar, V.P. Venugopalan, and Sunil K. Ghosh

19

Development of Eco-friendly Biopesticide Formulation for Mosquito Larvae Control

Ashok B. Hadapad, Arpit Prashar, Vikas, Ramesh S. Hire, Omkar Kinkar and Ravindra D. Makde

24

Nobel Prize 2020 in Physics

Dr. Subir Bhattacharyya

This page is intentionally left blank

Titanium Hydride targets for Portable Neutron Generator applications

Mayank Shukla*, Niranjan Ramgir, Prashant Singh, Yogesh Kashyap,
A. K. Debnath, K. P. Muthe, Tushar Roy, Baribaddala Ravi and Shefali Shukla

Technical Physics Division, Physics Group

S. G. Sawant, S. K. Raut, Ram Avtar Jat and S. C. Parida

Product Development Division, Radiochemistry & Isotope Group

K. G. Bhushan and K. C. Rao

Electromagnetic Application and Instrumentation Division, Physics Group

Abstract

We present the work on development of copper (Cu) substrate based thin film titanium (Ti) hydride targets for neutron generators. These targets have been specifically developed for portable neutron generators that find application in detection of special nuclear materials and explosives, detector calibration and the industrial neutron radiography. In the light of these select applications and the restrictive monopoly of foreign suppliers, this import substitute technology assumes critical significance as these targets are consumable and need to be replaced after a few hundred hours of operation in a neutron generator. Thermal vapor deposition followed by chemi-adsorption of deuterium (D) or tritium (T) has been used to produce thin film titanium hydride (TiD_x and TiT_x). These D and T loaded targets have given neutron yield of $\sim 10^6$ and $\sim 10^8$ n/s, respectively in an indigenously developed portable neutron generator.

Keywords: Titanium hydride targets, deuterium, tritium, neutron yield, portable neutron generator

Introduction

DC accelerator based neutron generators, in particular portable neutron generators (PNG) besides having applications in areas, including detection of special nuclear materials, explosive detection, narcotics detection, neutron radiography are also extensively used in oil well logging, mining exploration, coal analysis for power plants, material characterization and prompt gamma neutron activation [1-7]. Small size PNG comprise of an ion source, compact linear DC accelerator and neutron producing target (TiD_x or TiT_x). In neutron generators, interaction of an accelerated D-ion beam with the target produces mono energetic neutrons through D-D (2.45 MeV) / D-T (14.1 MeV) fusion reaction. The neutron target usually consists of few micron thick metallic getter film deposited on a metallic substrate of high thermal

conductivity. This getter film is then exposed to deuterium or tritium gas, thereby forming an active metal hydride neutron producing layer. In order to get a stable neutron output in a neutron generator, the neutron producing target should possess properties such as high thermal stability, high hydrogen isotope storage capacity, mechanical stability under energetic particle interaction and high heat conductivity besides the ease of fabrication. Thin films of Titanium, Zirconium, Vanadium, Hafnium, Niobium, Lithium, Lanthanum, Yttrium, or Thorium as well as various alloys have been widely used in storage of hydrogen and its isotopes by researchers [8]. Amongst these, Ti has been found to be a material of choice for neutron targets as it is economical, ability to withstand high temperatures and hydrogen isotope storage capacity (H/Ti) as high as 2, which gives a high

neutron yield. However, development of these getter films is one of the technological challenges. In this work, we report development of these targets by depositing $\sim 3.5\mu\text{m}$ Ti film on 16mm diameter Cu-substrate, using thermal vapor deposition.

Deposition of Ti films

Owing to its high thermal conductivity and ease of machinability, oxygen free high conducting (OFHC) copper was chosen as a substrate material for preparation of targets. Copper (Cu) discs of 16 mm diameter and 0.6 mm thickness were cut from a pre-fabricated rod of similar diameter. These discs were polished, cleaned physically first and later using ultrasonic cleaner prior to deposition to avoid any surface contamination. Thermal vapor deposition method was used to deposit a uniform Ti thin film onto the Cu substrate. This method was chosen over other methods such

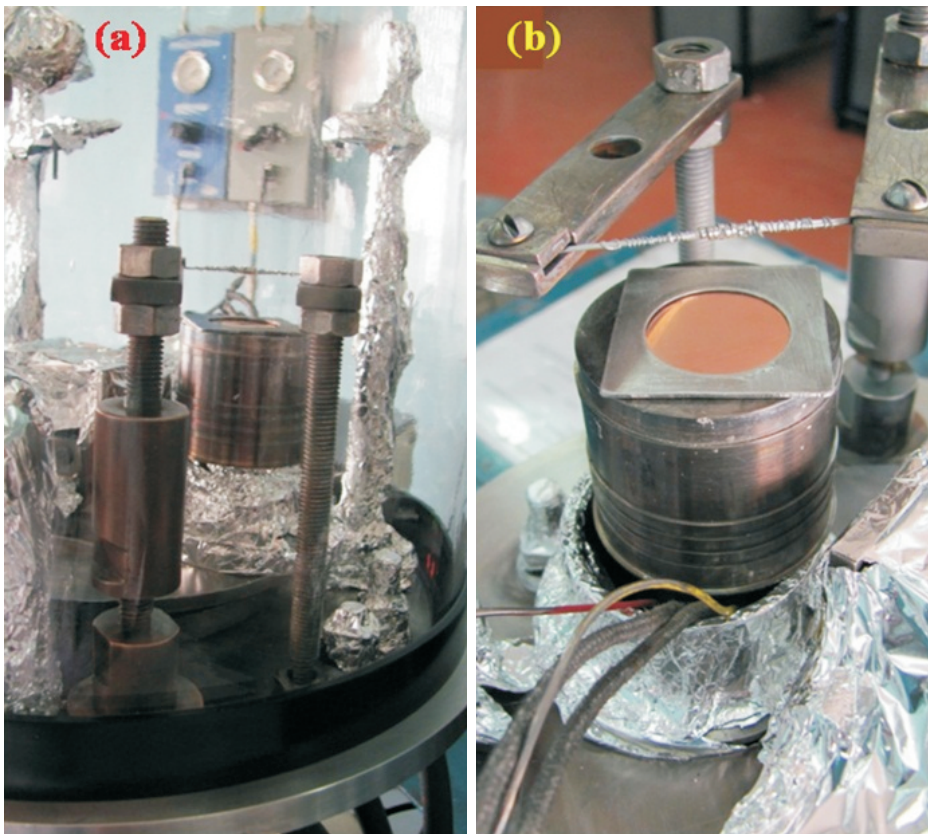


Fig. 1: (a) Deposition arrangement inside thermal evaporator, and (b) zoomed image showing the filament and the heater containing the Cu disc with SS mask

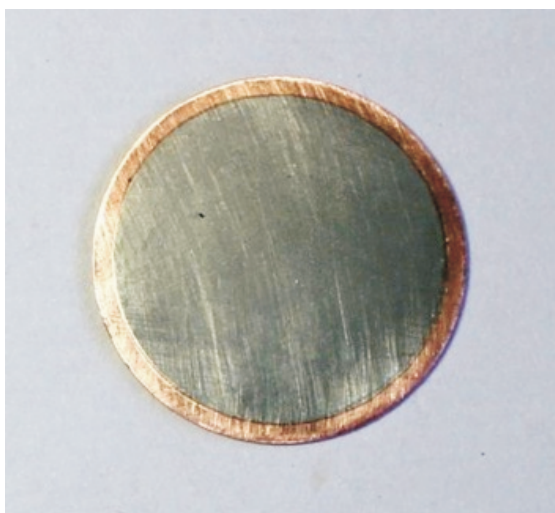


Fig. 2: Deposited Ti layer (3.5µm) on Copper Target

as DC or RF sputtering, as it offers required thickness (in micrometers) in a few hours time, besides being quite economical. Fig.1a shows the mounting set-up, Ti wire loaded tungsten (W) filament and Cu disc

with stainless steel (SS) mask inside the bell jar of thermal evaporator. A close-up view of the same is shown in Fig.1b. The melting point of Ti is 1668°C and in the physical vapor deposition using W-filament, it is

possible to generate temperature close to 1800°C, thereby ensuring evaporation of Ti. Thickness of the deposited film was estimated by weight difference method using an ultra-precision weighing balance of least count 0.1 mg. Fig.2 shows the as-deposited Ti film on the Cu substrate. The greyish colour of the deposited film indicates metallic nature of the deposited material.

Ti getter film characterization

The quality of a film is determined by uniformity of the deposited layer, good adhesion to the substrate above the activation temperature and low absorption of residual gas (mainly oxygen). The developed Ti film was characterized by employing Scanning Electron Microscopy (SEM), X-ray Photoelectron Spectroscopy (XPS) studies and by estimating the amount of absorbed residual gas using Residual Gas Analyzer (RGA) [9]. SEM studies were predominantly carried out to determine the uniformity of microstructure of the deposited film.

The cross-sectional and lateral SEM image as shown in Fig.3 indicate the overall uniform deposition and >95% of solid density of Ti (4.506 gm/cc). During cooling cycle in the evaporator system, it is likely that the Ti may pick up the oxygen and form Titanium oxide. To confirm the presence of oxygen, XPS measurements were carried out using Mg-K_α (1253.6 eV) source. Fig.4 shows the Ti-2p and O-1s spectra for as-deposited Ti films on the Cu discs. The measured peaks indicate that the deposited film has Ti/TiO_x composition top surface up to 20 nm along with possible excessive adsorbed oxygen. The amount of dissolved oxygen in the deposited Ti-films was determined using RGA at vacuum level of ~10⁻⁷ mbar and substrate temperature of ~100°C. The oxygen out-gassing curve recorded for bare and Ti deposited Cu substrate is

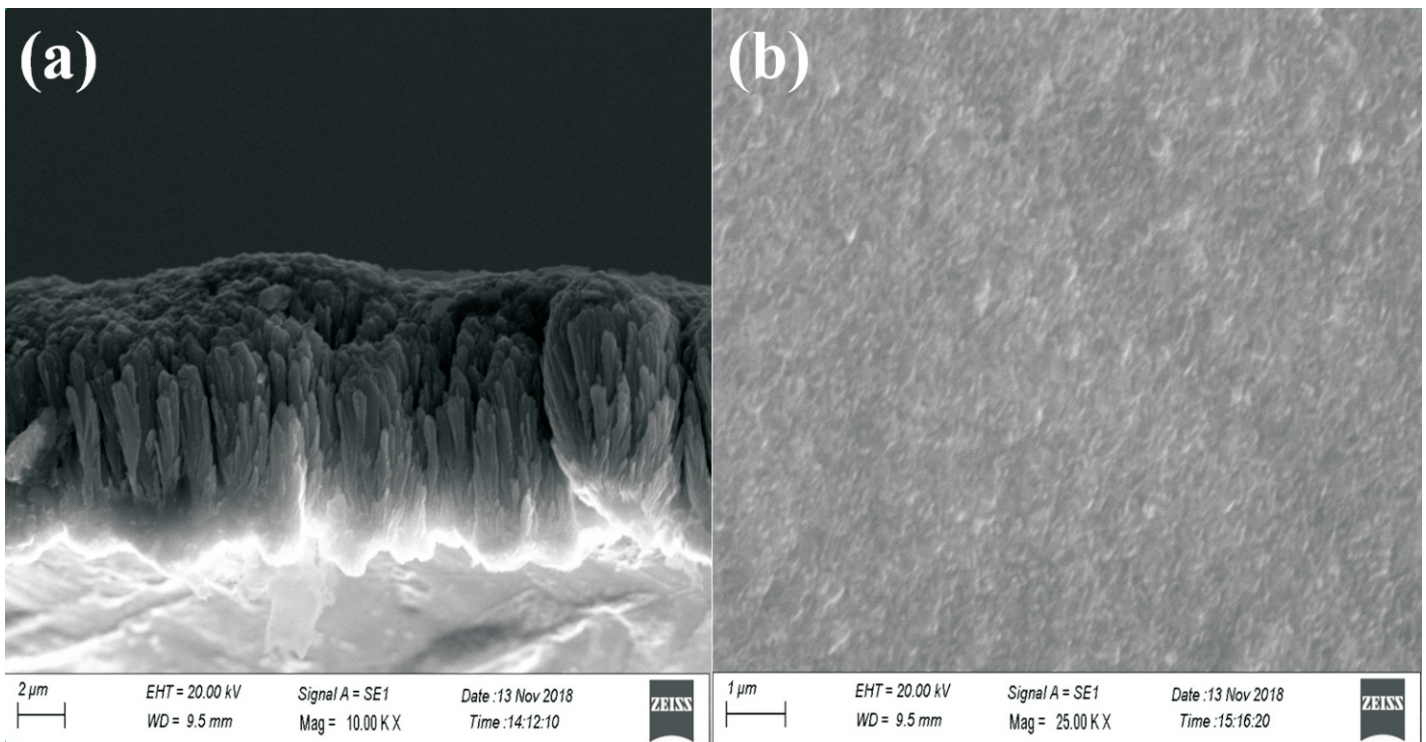


Fig. 3: SEM Snapshots of deposited Ti layer showing uniformity

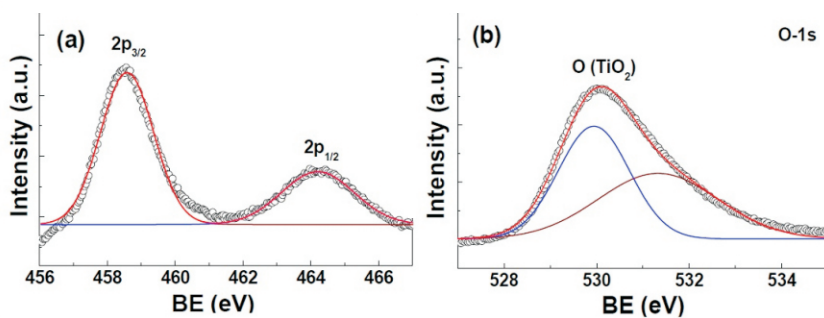


Fig. 4: Ti-2p and O-1s spectra for Ti films on OFHC Cu discs (a) and (b) respectively

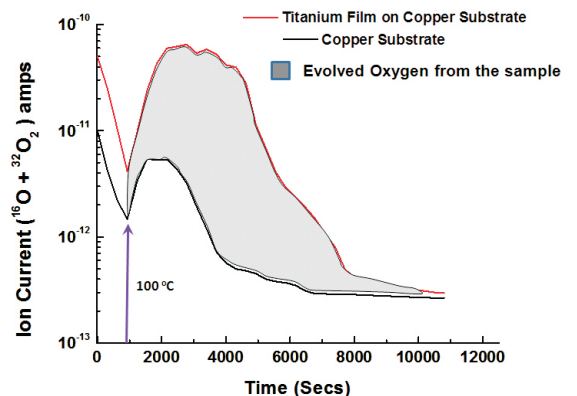


Fig. 5: Oxygen out-gassing curves for bare copper sample and Titanium film coated sample

shown in Fig.5. Extra dissolved oxygen of ~ 470 ppm ($\pm 10\%$) was measured for Ti deposited Cu substrate as compared to bare Cu, thereby confirming the good quality of the Ti films. Importantly, the deposited film offered a service temperature of up to 500°C , a clear indication that the film doesn't peel off up to this temperature, which is a necessary prerequisite for their application as neutron generators.

Loading of hydrogen isotope in Ti film

Hydrogen isotopes (D or T) loading in the Ti ($\sim 3.5\mu\text{m}$) thin films targets were carried out using indigenously designed and fabricated ultra-high vacuum (UHV) gas handling manifold installed inside an inert atmosphere glove box. The UHV system consists of reaction vessel, pre-calibrated volumes, pressure and vacuum gauges and turbo molecular pumping station.

Prior to loading of hydrogen isotopes, the Ti target was activated by heating it up to 500°C under high vacuum conditions and the activated Ti target was exposed to hydrogen isotopes. The system pressure was monitored and the hydrogen isotope concentration in Ti target was calculated by employing pressure-volume relationship. The final composition of the TiQ_x ($Q = \text{H or D}$) phase was calculated from the final

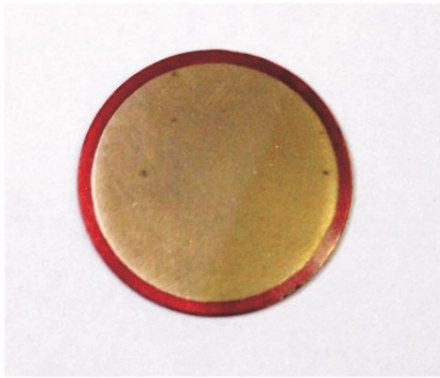


Fig. 6a: Deuterium target



Fig. 6b: Tritium Target

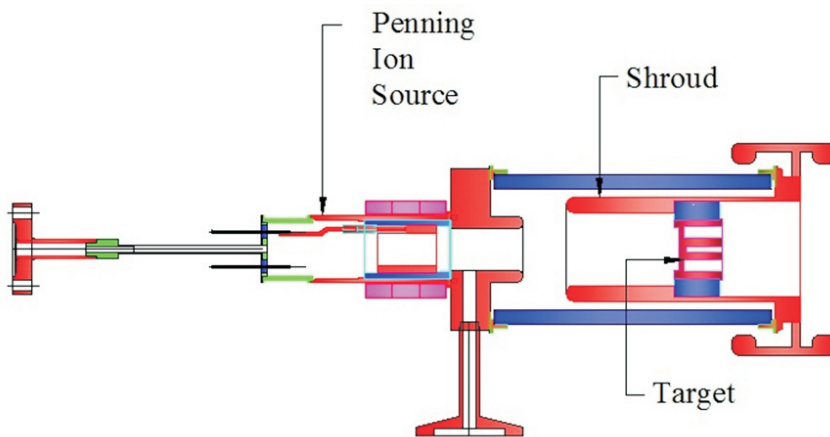


Fig. 7: Portable Neutron Generator Schematic



Fig. 8: Neutron generated bubbles in a bubble detector from deuterium target in D-D mode

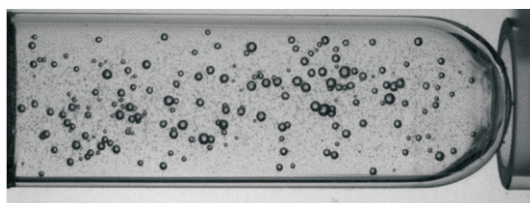


Fig. 9: Neutron generated bubbles imaged using bubble detector reader for yield estimation from tritium target in D-T mode

pressure of the system. For 3.5µm thick Ti film of 12mm diameter, and volume of $\sim 4 \times 10^{-4}$ cc, deposited on 16 mm diameter Cu substrate, the amount of deuterium loading was found to be 2.1 ($\pm 10\%$) standard cubic centimeters (scc). Similarly, tritium loaded target was found to have an activity of ~ 3 Ci ($\pm 10\%$) for the same thickness of Ti. Calorimetric results were corroborated with the composition calculated from the pressure-volume relationship. Fig.6a & Fig.6b show the physical appearance of D & T loaded targets, respectively.

Testing of targets in portable neutron generator

The Titanium-hydride targets (both TiD_x & TiT_x) were tested in an indigenously developed portable neutron generator. Fig.7 shows the schematic and the photograph of the generator assembly. It consists of a miniature penning ion source, a suppression metallic shroud and an externally cooled target holding assembly put together in proximity focused triode geometry. Gas insertion in the ion chamber from a gas cylinder was controlled using precision gas dosi-valve. The penning ion source was operated at deuterium gas pressure of $\sim 2 \times 10^{-5}$ mbar using 0-3 kV DC power supply. The D^+ ion beam was extracted through an aperture and accelerated up to ~ 80 kV DC before their interaction with the target material. In this generator, the target electrode was maintained to a high negative potential (-80 kV) and the ion source at ground potential. The high energy ion beam hits the solid neutron target to produce fusion neutrons. Fig.8 shows the neutron generated bubbles in a bubble detector from the D-target in D-D mode. The neutron yield was estimated by counting the number of bubbles, detector sensitivity and dose equivalent for D-D (2.45MeV)/D-T(14.1MeV) neutrons [10].Fig.9

shows neutron generated bubbles from T-target in D-T mode using a bubble detector reader. In case of deuterium target, the neutron yield was estimated to be $\sim 10^6$ n/s, whereas for the tritium target it was estimated to be $\sim 10^8$ n/s.

Conclusion

A process for fabrication of Titanium hydride (TiD_x & TiT_x) targets on Cu substrates for portable neutron generator application has been successfully designed, developed, rigorously tested and validated. Excellent quality Titanium getter films of highly preferred thickness of $\sim 3.5\mu m$, having good adherence and service temperature of $\sim 500^\circ C$ were deposited using thermal vapor deposition technique on a Cu substrate. For a $3.5\mu m$ thick and 12mm diameter Titanium film with active volume of $\sim 4 \times 10^{-4} cc$ deposited on 16mm diameter Cu substrate, deuterium loading of 2.1 ($\pm 10\%$) standard cubic centimeters (scc) was achieved, and this target provided a neutron yield of $\sim 10^6$ n/s in an indigenously developed portable neutron generator. Similarly, $\sim 3 Ci$ ($\pm 10\%$) activity of tritium was achieved for the same Ti thickness resulting in a neutron yield of $\sim 10^8$ n/s. Moreover, thermal vapor deposition system was also suitably modified and optimized to obtain Titanium films of up to 35 mm diameter (active layer). Efforts are in progress for developing of Ti films having thickness of $10\mu m$, which can potentially result in targets for high yield ($\sim 10^{10}$ n/s) neutron generator applications.

*Corresponding author

Dr. Mayank Shukla

Acknowledgements

Authors are thankful to Dr. T. V. Chandrasekhar Rao, Head, Technical Physics Division and Dr. P. K. Pujari, Director, RC&I Group for his support. We would also like to thank Dr. P. K. Patro, Powder Metallurgy Division for assisting in SEM characterization.

References

1. "Neutron Generators for Analytical Purposes", IAEA Radiation Technology Reports Series No. 1, 2012.
2. "Compact Neutron Generators for Medical, Home Land, Security and Planetary Exploration", J. Reijonen, E.O. Lawrence, Proc. Particle Accelerator Conference, Knoxville, Tennessee, 2005.
3. "Development of a Compact Neutron Generator to be Used for Associated Particle Imaging using a RF-Driven Ion Source", Y. Wu, Ph.D. thesis, University of California, Berkeley, 2009.
4. "Development of miniature neutron generators for science and well logging", E. S. Grishnyaev, 4th Asian Forum for Accelerators and Detectors (AFAD -2013), February 25-26, 2013, Novosibirsk, Russia.
5. "Neutron Interrogation to Identify Chemical Elements with an Ion-Tube Neutron Source", Alvarez, R. A.; Dougan, A. D.; Rowland, M. R.; Wang, T. F., J. Radioanal. Nucl. Chem. 1995, 192, 73-80.

6. "Non-Destructive Characterization using Pulsed Fast-Thermal Neutrons", P. C. Womble, F. J. Schultz, G. Vourvopoulos, Nucl. Instrum. Methods Physics Res. B 1995, 99, 757-760.
7. "Advances in Neutron Based Bulk Explosive Detection", T. Gozani, D. Strellis, Nucl. Instrum. Methods Physics Res. B, 261 (2007), 1-2, pp.311-315.
8. "Differential Die Away Analysis for detection of ^{235}U in a metallic matrix", Y. Kashyap, A. Agrawal, T. Roy, P. S. Sarkar, M. Shukla, T. Patel, A. Sinha, Nucl. Instrum. Methods Physics Res. A, 806B, 2016, pp. 1-4.
9. "Indigenous Development of Neutron Producing Targets for DC Accelerator based Neutron Generators", Mayank Shukla, Niranjana Ramgir, Baribaddala Ravi, Prashant Singh, K. R. Sinju, A. K. Debnath, K. P. Muthe, Yogesh Kashyap, Tushar Roy, Shefali Shukla, Mahendra More, K. G. Bhushan, K. C. Rao, S. G. Sawant, Ram Avtar Jat, S. K. Raut, S. C. Parida, S. C. Gadkari and T.V. Chandrasekhar Rao, BARC Internal Report, BARC/2020/I/006.
10. "Impact of Switching to the ICRP-74, Neutron Flux-to-Dose Equivalent Rate Conversion Factors at the Sandia National Laboratory Building 818 Neutron Source Range", Sandia Report, D. C. Ward, Sandia National Laboratories, Albuquerque, N. Mex., USA, SAND2009-1144, 2009.

Plasma Pyrolysis and Incineration for Low Level Radioactive Solid Wastes

K. C. Pancholi*, C. P. Kaushik*

Homi Bhabha National Institute, Mumbai-400094

Suprabha, S. Agarwal, S. K. Solankar, S. K. Mishra, N. S. Tomar, C. P. Kaushik

Nuclear Recycle Group, BARC, Trombay, Mumbai-400085

S. Bhandari, S. Ghorui, R. L. Bhardwaj, E. Kandaswamy, M. Martin, A. Sharma

Beam Technology Development Group, BARC, Trombay, Mumbai-400085

Abstract

Low level solid wastes (≤ 2 mGy/hr) are managed either by compaction or incineration. Cellulosic wastes undergo incineration to offer a volume reduction factor of 30-50, whereas rubber and plastic wastes are compacted to give a volume reduction factor of about 3. Conventional incineration of such wastes releases toxic gases, viz. Dioxin and Furan. High temperature plasma process is internationally accepted as an effective solution for incineration of all types of combustible wastes. The exhaust emissions out of this process are well within the standards prescribed by government agencies. The present article provides a brief account of efforts to demonstrate plasma based technology for management of all types of potentially combustible radioactive solid wastes. The 25kg/hr-capacity-system designed to carry out this activity has been equipped to treat wastes in a single step at a very high temperature (> 1500 K). Experience gained during the demonstration runs would help in scaling the system's capacity significantly higher to treat 50 kg/hr. The scaled-up version could see immediate deployment across several DAE facilities besides having potential applications for managing municipal wastes upwards of 100 tons per day.

Keywords: High temperature plasma process for pyrolysis and incineration, Plasma Chamber, Low Level Radioactive Solid Wastes, Volume Reduction Factor (VRF), Cu-Hf torch, Graphite torch, Compaction, Incineration, Combustible Wastes, Dioxin, Furan, Nuclear Recycle Group

Introduction

Nuclear energy/radiation facilities generate secondary solid wastes during their day-to-day operation and maintenance (O&M) activities, which may cause potential radioactive contamination [1]. These radioactive wastes are classified into six categories viz. 1) Exempt waste 2) Very short lived waste 3) Very low level waste 4) Low level waste, 5) Intermediate level waste and 6) High level waste, mostly based on the level of radioactive contamination and disposal requirements [2]. Solid wastes with low level of radioactivity require pre-disposal management for volume reduction [3]. In BARC Trombay, low level solid wastes (≤ 2 mGy/h) originating from O&M of various

facilities have rubber, plastics and ventilation filters, which constitute more than 70% of total volume [3,4].

For volume reduction of waste prior to their disposal in the Near Surface Disposal Facility, cellulosic waste is incinerated using oil/diesel-fired incinerator whereas rubber, plastics and ventilation filters are usually compacted [4,5]. Incineration results in very high Volume Reduction Factor (VRF) of 30-50, whereas compaction leads to relatively much lower VRF of 3-5 [4,5]. Incineration of rubber and plastic wastes by use of conventional fuel-fired incinerators is not highly preferred due to generation of toxic gases like dioxins and furans due to lower operating temperatures [6,7]. Of late, advancements in plasma-based technology for pyrolysis/incineration

showed good promise, and the technology may be applied for the management of combustible wastes, as high-temperature plasma substantially reduces formation of dioxins and furans [7,8,9].

In the past the Institute of Plasma Research (IPR) had successfully demonstrated the working of graphite-based plasma system, and deployed it for management of medical waste and domestic waste [10]. Therefore, plasma-based pyrolysis/incineration of combustible, low level radioactive solid wastes see high level of volume reduction, and the approach is eco-friendly because dioxins, furans and poly aromatic hydrocarbons in the exhaust gas are well within the prescribed norms for emission.

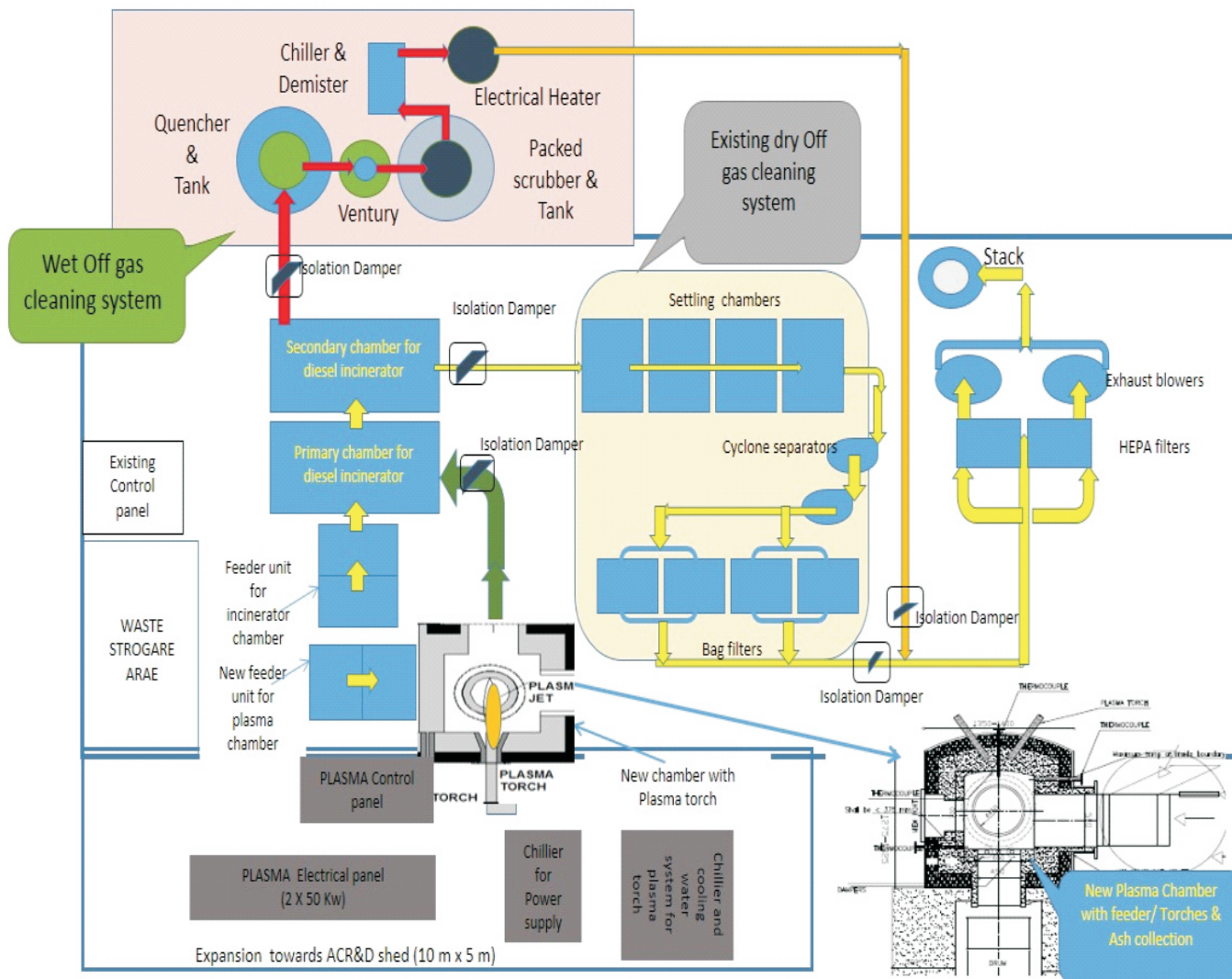


Fig. 1: Layout of plasma pyrolysis and incineration demonstration facility

Development of plasma pyrolyzer and incineration demonstration facility

In order to demonstrate the advantages of high temperature process, it was decided to integrate a plasma pyrolyser prior to the existing fuel-fired incinerator as shown in Fig. 1 [11,12]. The existing incineration facility comprises of fuel-fired primary and secondary combustion chambers, settling chamber, cyclone separators, bag filters, HEPA filters, blower and stack. A plasma pyrolyser was retrofitted into the existing system such that the gaseous products from the pyrolyser can be directed to primary chamber followed by the secondary chamber for combustion. From the readily available plasma

technologies of DAE, a non-transferred atmospheric type of plasma was selected for pyrolysis. The pyrolyser is provided with two types of plasma systems - metal electrodes and graphite electrodes. The pyrolyser has been designed to process 25 kg/hr [12].

The retrofitted plasma demonstration set-up has following components:

- a) New dedicated plasma chamber,
- b) A dedicated waste feeder unit with upgraded design
- c) 10 TR and 5 TR Chillers for cooling needs & associated piping and services
- d) Interconnecting duct between new chamber and existing incinerator

combustion chamber with isolation damper

- e) 100 kW power supply (50 kW+ 50kW)
- f) Two type of plasma system of 30 kW rating each viz.
 - (i) Graphite electrodes (1 Cathode + 2 Anode) – placed in inverted tripod configuration
 - (ii) Metal electrode (Cu + Hf) torch (developed by L&PTD, BARC) - horizontally placed

Testing and commissioning activities

The system was tested and commissioned with simulated waste in January 2018. About 400 kg of simulated waste comprising of

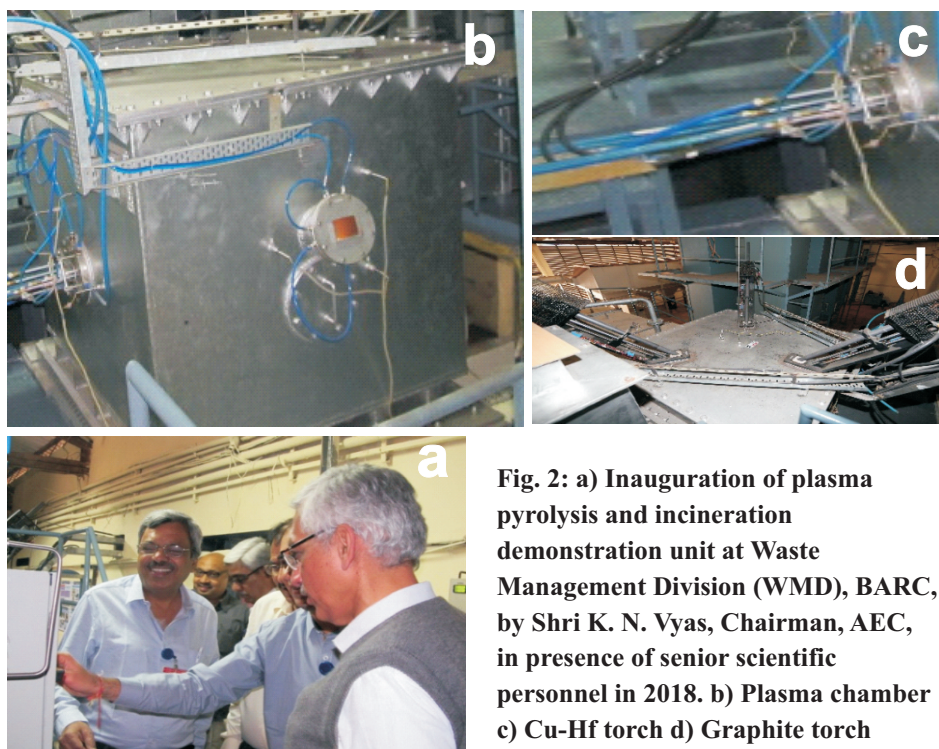


Fig. 2: a) Inauguration of plasma pyrolysis and incineration demonstration unit at Waste Management Division (WMD), BARC, by Shri K. N. Vyas, Chairman, AEC, in presence of senior scientific personnel in 2018. b) Plasma chamber c) Cu-Hf torch d) Graphite torch

cellulosic, rubber & plastic waste and mixed wastes was treated in about 10 trial runs (6 runs with L&PTD torch and 4 runs with Graphite torch). Operation parameters in both systems were found to be satisfactory.

Parameters during testing trials were noted as reference for actual active runs. Necessary feedback with respect to both plasma systems was enlisted for performance enhancement and improvements in safety aspects. Detailed analysis led to necessary design change in the original Cu-Hf torch to achieve stable performance. The action-taken report on the recommendations was also reviewed by safety committee along with the feedback of inactive trials. It was decided to take up continuous trails with Cu-Hf based torch and Graphite electrode based system was employed as a stand-by unit.

After obtaining necessary clearances from the safety committee, the system was hot commissioned on September 19, 2018 for plasma demonstration system at RSMS, WMD, NRG, facilities by using Cu-Hf based torch. The system successfully processed

more than 1200 kgs of potentially active wastes (0.2-5 mR/hr). Feedback of several batches amounting to processing of 125 nos. of 64L cardboard boxes (3-18 kg per box range) has been summarized for future studies.

Location of various thermocouples is shown in Fig. 3. All active trial runs completed at rated capacity successfully. Observations are enlisted as follows.

- Four runs were conducted, in batch of 35-100kg actual active cellulosic wastes with < 5% plastic content processing 300 kg wastes of 0.2-2 mR/hr contact dose.
- Two runs with mixed wastes (~70% cellulosic and ~30% rubber and plastic) with contact dose of 0.5-1 mR/hr were carried out. The waste here was the rejected personal protective wears from Decontamination Centre, WMD.
- A solitary run was conducted with about 100 kg of cellulosic waste with < 5% plastic content and having 3-5 mR/hr contact dose. The waste was collected from PP and WIP in BARC.

- Two runs of round-the-clock operation, of actual active cellulosic wastes with < 5% plastic content and having contact dose 0.2-2 mR/hr, processing more than 500 kg wastes.

Brief summary of the active runs is listed below.

Torch operational duration (continuous in a trial run/ Total): 22 hr/85hr.

Waste feeding duration (continuous in a trail run/ Total): 18hr/50hr.

Waste feed rate in all trail runs: 18-25 kg/hr

Temperature (Max) achieved in plasma chamber gas space: 1350 °C

Temperature (Max) for the chamber wall :1300 °C

Temperature (Max) in the flue gas combustion chamber: 950 °C

Operation of torches and power supply : Satisfactory

Operation of feeder unit: Satisfactory

Waste to Residue ash ratio: >30 (v/v) or >18 (w/w)

Radiological discharges through flue gases: BDL

Discharge gas composition (CO, NO_x, Co₂, etc.): Within Limits

Key observations and Future course

Upgradation of flue gas management with wet type system is in progress (Fig. 1). This will ensure prevention of formation of Dioxin and Furans by recombination as well as removal of hazardous gases by scrubbing. Utilizing the experience gained out of operating the facility, a 50 kg/hr

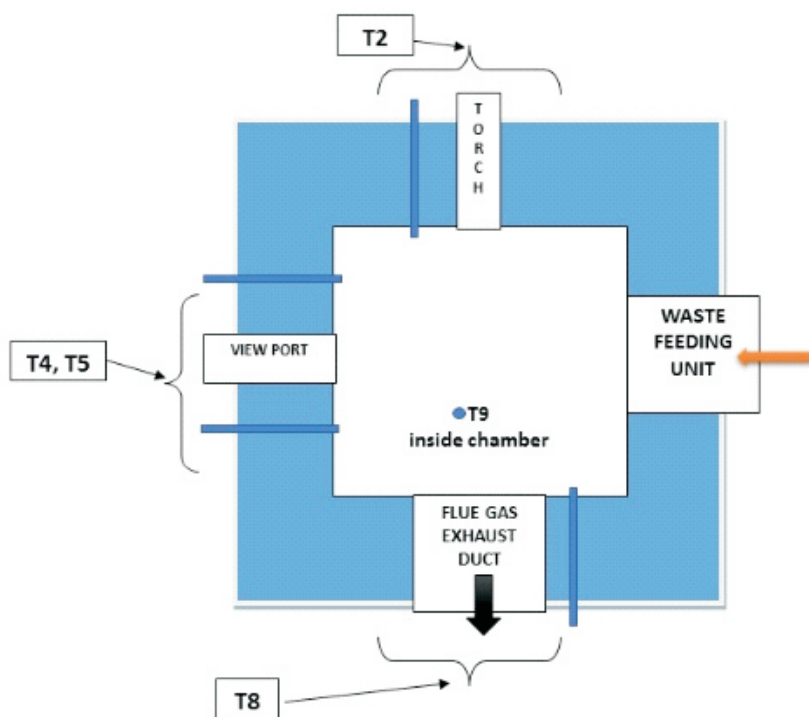


Fig. 3: Typical plan of chamber with thermocouple locations

capacity plant is being standardized for deployment in most of the DAE facilities to deal with low level radioactive solid waste management. Based on the feedback obtained from demonstration runs, an optimized multi-torch based higher capacity (25 TPD) system is being designed in BARC jointly by WMD, L&PTD and Institute of Plasma Research (IPR), Gandhinagar for municipal waste management. It must be noted IPR and L&PTD had already initiated work on upgrading their plasma torch capacity. Besides this, IPR also started a simulation study on plasma chamber for understanding temperature distribution inside the plasma chamber. Establishment of sampling and analysis of Dioxin and Furans within BARC set-up is underway by Nuclear Recycle Group & Chemistry Group through a joint collaboration with CSIR-National Environmental Engineering Research Institute.

Important observations

As Graphite is a fragile material, measures had been incorporated to avoid its direct contact with the

radioactive waste box. Sustained operation of plasma generating systems required frequent intervention of system operators. Flue gases exiting from plasma chamber, with temperature above 500°C, showed complete combustion of CO to CO₂ in after-burner chamber. The CO discharges were observed to be within the prescribed limit. The density of waste packed into the box has a direct bearing on the rate of processing as well as on the temperature of flue gas exiting from the pyrolysis chamber.

Conclusion

Plasma pyrolysis and incineration is the ideal approach for safe management of all forms of low level combustible wastes with a negligible impact on the environment. Plasma for low level waste management is an evolving technology and has given satisfactory performance in the test conditions. New technological advancements are under progress for achieving operational robustness. For ensuring better performance of the graphite based system, a horizontal 'T'

shape based configuration with inert gas purge is desirable for better stability of plasma plume. This configuration is mostly preferred as it provides better control over the movement of graphite rod. A single box with 5-8 kg of waste and optimum packing density is ideal for adequate waste processing.

*Corresponding authors:

Shri K.C. Pancholi, Dr. C.P. Kaushik

Acknowledgement

Authors deeply acknowledge the encouragement and valuable guidance provided by Shri R. K. Rajawat, Shri K. Agarwal, Shri P. K. Wattal and late Dr. Sekhar Basu throughout the course of work on this first-of-its-kind project. Authors convey heartfelt thanks to Shri A. Shirole, Shri Ramakant, Shri N. R. Ranade, Shri D. N. Patil, Shri K. J. Pawar, Shri A. Shanmugam and Shri D. K. Baskey for their technical contribution towards successful demonstration of the technology set-up. Thanks to teams from NRG and BTDG for their valuable contribution during several pilot runs of the system.

References

1. Sant'ana L. P. and Cordeiro T., "Management of radioactive waste: A review", in Proceedings of the International Academy of Ecology and Environmental Sciences, 6: p38-43 (2016).
2. International Atomic Energy Agency (IAEA), General Safety Guide GSG-1, "Classification of radioactive waste", Vienna (2009).
3. International Atomic Energy Agency (IAEA), Specific Safety Guide, SSG-40, "Predisposal management of radioactive waste from nuclear power plants and research reactors", Vienna (2016).
4. Raj K., Prasad K. K. and Bansal N. K., "Radioactive waste

- management practices in India”, Nuclear Engineering and Design, Volume 236, Issues 7–8, p914-930 (April, 2006).
5. Wattal P. K., “Indian programme on radioactive waste management”, Indian Academy of Sciences, Vol. 38, Part 5, p849–857 (October, 2013).
 6. Fiedler H., “Dioxins and furans (PCDD/PCDF)”, Persistent Organic Pollutants- The Handbook of Environmental Chemistry (Vol. 3.O), Springer, p123-201(2003).
 7. Incineration and Dioxins: Review of Formation Process, Consultancy report prepared by Environmental and Safety Services for Environment Australia, Commonwealth Department of the Environment and Heritage, Canberra, Available at: <https://www.environment.gov.au/protection/publications/incineration-and-dioxins-review-formation-processes> (1999).
 8. International Atomic Energy Agency (IAEA), Tech Doc series no 1527, “Application of thermal technologies for processing of radioactive waste”, Vienna (2006).
 9. Prado E. S., Miranda F. S., de Araujo L. G., Petraconi G. and Baldan M. R., “Thermal plasma technology for radioactive waste treatment: a review”, Journal of Radioanalytical and Nuclear Chemistry, p 1-12 (2020).
 10. Nema S. and Ganeshprasad K., “Plasma pyrolysis of medical waste”, Current science, p 271-278 (2002).
 11. Pancholi K. C., Agarwal S., Solankar S. K., Pol S. K., Patil D. N., Tomar N. S., Kaushik C. P. “Study on the mechanism of the waste box incineration in the conventional waste incinerator installed at RSMS, WMD, BARC”, Proceeding of the DAE-BRNS 7th Interdisciplinary Symposium on Materials Chemistry, Mumbai, p 156 (2018).
 12. Pancholi K. C., Kumar K., Pol S., Jain S., Rakesh R. R., Maniyar P. D., Agarwal K., “Challenges and Innovations in Management & Disposal of Radioactive Solid Wastes at Trombay”, Proceedings of International Conference on Radioactive Waste Management in India, p 53-54 (2019).

Affordable [¹⁸F] FLT Precursors for PET Imaging

K. S. Ajish Kumar*, V. P. Venugopalan, and Sunil K. Ghosh

Bio-Organic Division, BARC

Abstract

The non-invasive positron emission tomography (PET) for imaging of biological processes is a highly sensitive technique for disease diagnosis as well as for monitoring of patient response to treatment. This technique works through harnessing the variation in metabolic disorders, like overexpression of certain antigen or extensive requirement of biomolecules like amino acids, glucose etc, found in the cancerous site of the human body. In terms of choosing the ideal PET radiotracer between [¹⁸F] Fluoro-2-deoxyglucose ([¹⁸F]FDG) and 3'-fluoro-L-3'-deoxythymidine ([¹⁸F]FLT), the latter is preferred as it is independent of glucose metabolism and because of this, there is no uptake of it in inflammatory cells and healthy brain tissues. More importantly, [¹⁸F] FLT ensures greater degree of efficiency in diagnosis, and acts as an alternative to [¹⁸F] FDG for its low sensitivity. A protocol for an efficient and economically viable synthesis of three [¹⁸F] FLT precursors from commercially available thymidine (as a starting material) was initiated in BARC as part of the efforts to indigenize highly expensive precursors that are presently being used. These in-house synthesised [¹⁸F] FLT precursors were characterized using multiple techniques, including Nuclear Magnetic Resonance (NMR), High Performance Liquid Chromatography (HPLC), Mass Spectrometry (MS), etc. The results obtained were highly encouraging and they were comparable to the commercially available sample.

Keywords: Radiopharmaceuticals, Fluorothymidine, Precursors, Diagnosis, In-house

Introduction

Extensive research in radiopharmaceuticals led to the development of numerous nuclear medicines for various human disorders, particularly to address malignancies arising due to uncontrolled cell division, commonly called as cancer. For an effective cancer treatment, availability of highly sensitive and specific modality for detection of malignancies in the early stages of the disease is very crucial. Nuclear medicine based imaging; specifically positron emission tomography (PET) provides an accurate picture of the distribution of disease in human body through high quality images of moderate to high resolution. PET is not only used to provide specific inputs on the disease but also renders vital information required for discovery of novel drugs. For e.g. PET can throw light on the possible side effects in the human body, if any, due to undesired

interactions of potential drug candidates, which are in the clinical trial stage.¹⁻⁴ Radionuclides such as ¹⁵O, ¹³N, ¹¹C, and ¹⁸F constitute few of the commonly used positron emitting radionuclides employed in the radiolabelling of synthetic analogues of natural molecules to form radiopharmaceuticals.

Amongst them, ¹⁸F with a relatively long half-life of 109.8 min, is ideal for PET based radiopharmaceuticals as it can be produced with greater ease (using cyclotron) and can be shipped at a short notice to nearby hospitals. Among PET based imaging agents, glucose derived [¹⁸F]FDG, which works by taking advantage of the extensive glucose metabolism in cancer tissues, is considered as “molecule of the millennium”. Although [¹⁸F]FDG is an important diagnostic nuclear medicine for various cancers, it is not a specific radiotracer for the imaging of malignancies. There are various

processes in the body and tissues where the demand for glucose is quite high and in those cases, [¹⁸F]FDG can generate potential false signals. For instance, brain functioning depends on glucose metabolism, also inflammatory cells and microphages too have high glucose metabolism rate. As a result, [¹⁸F]FDG may easily accumulate in undesired cells or body parts alongside tumour cells. Hence uptake of [¹⁸F]FDG does not always reflect presence of tumour or its aggressiveness.⁵ This observation provided the impetus to initiate work on alternate radiopharmaceuticals whose mechanism of action is linked to cell division. This naturally directed chemists towards the discovery of nucleic acid based radiopharmaceuticals (e.g.; thymidine 1, Fig. 1). Since thymidine is involved in the synthesis phase (S-phase) of cell cycle⁶, radio-labelled thymidine received much focus during the search for new radiopharmaceuticals. The first radio-labelled thymidine

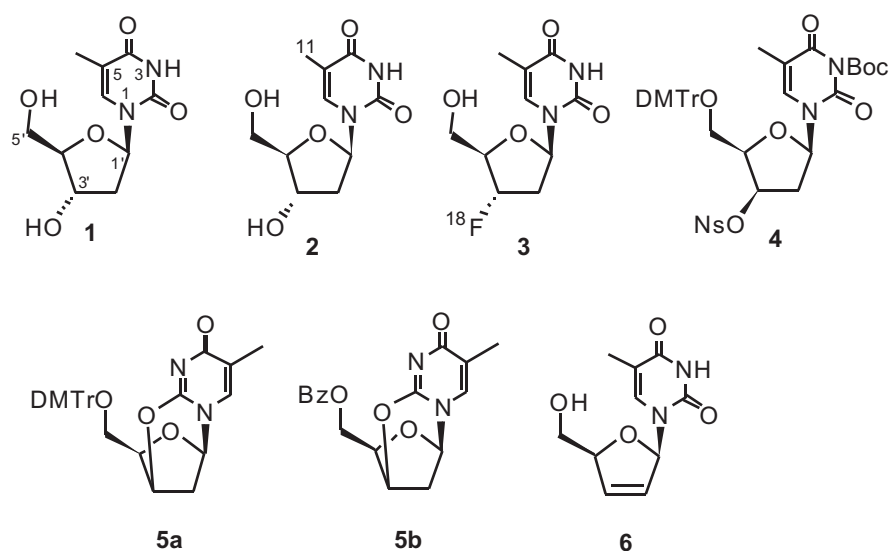


Fig. 1: Thymidine (1), [¹¹C]thymidine (2), [¹⁸F]FLT (3) and [¹⁸F]FLT precursors (4/5a/5b), Stavudine (6)

developed for imaging proliferation in vivo using PET was [¹¹C]thymidine (2, Fig. 1).⁷ Although [¹¹C] labelled thymidine turned out to be a useful imaging agent,⁸⁻¹¹ difficulty in development of images from the metabolite data coupled with its challenging synthesis dampened its global acceptance.

In order to overcome the shortcomings in [¹¹C]thymidine, the analogue of thymidine, 3-deoxy-3'-[¹⁸F]fluorothymidine, ([¹⁸F]FLT (3); Fig. 1) was developed.¹² FLT was initially developed as a thymidine analogue against HIV virus¹³⁻¹⁵ but Shields et al.¹⁶ demonstrated the use of [¹⁸F]FLT as a tumor proliferation marker in vivo. Unlike [¹¹C]thymidine, synthesis and handling of [¹⁸F]FLT is easy due to various aspects, including longer half-life of ¹⁸F, stability towards metabolic degradation, and its easy recognition by the proliferating cells.^{17,18} Importantly, [¹⁸F]FLT is stable to catabolism in vivo and has a simpler radio-synthesis. Bio-mechanistically, both FLT and thymidine are initially mono-phosphorylated in vivo by an enzyme called as thymidine kinase-1 (TK1), expressed during the DNA S-phase of the cell cycle.^{19,20} Cells in S-phase of

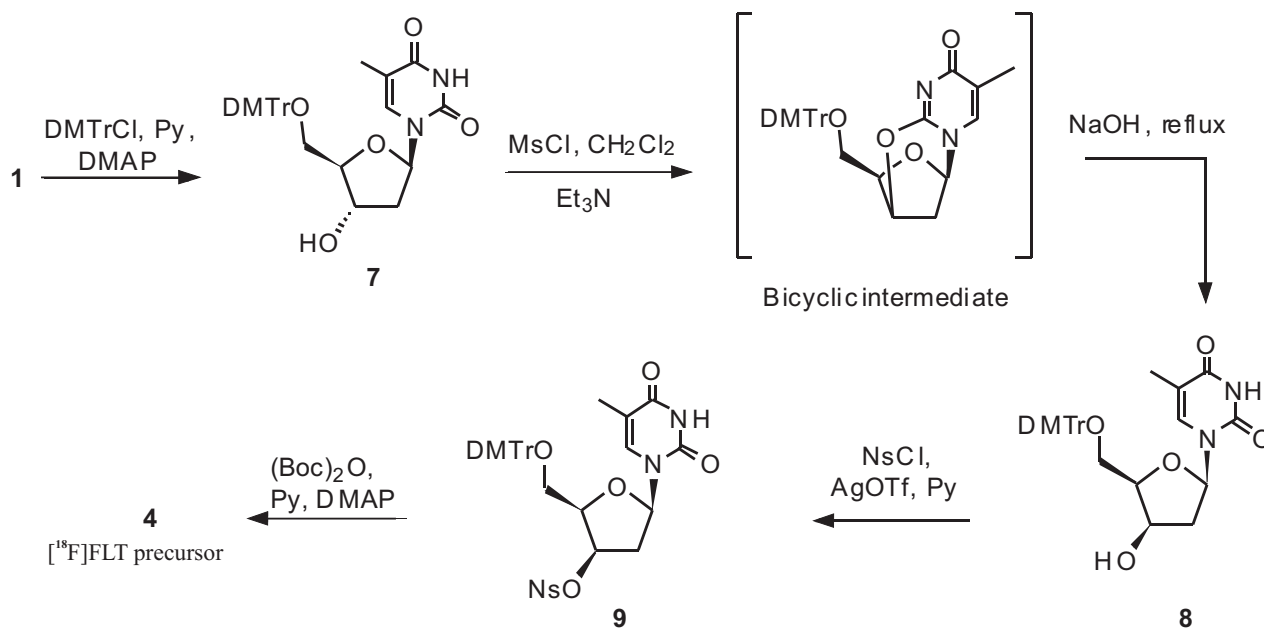
the cell cycle have TK1 in excess of 15-fold compared to other phases,¹⁹ and also its activity is optimal in cancer cells. Hence phosphorylation of thymidine in S-phase of cell cycle is an efficient process. While mono-phosphate derivative of thymidine is taken up by cells during DNA synthesis, mono-phosphates of [¹⁸F]FLT accrue as a cell membrane impervious species and can function as a sensitive and specific agent for imaging cellular proliferation.^{16,21} Moreover, the inherent capability of [¹⁸F]FLT to resist catabolism makes it a good imaging agent for a longer duration and gives a better signal-to-noise level. Additionally, [¹⁸F]FLT has the ability to discriminate benign and malignant adrenal tumors²² and also has standard uptake value which is two-fold in comparison to [¹¹C]Thymidine at 60 min in dog marrow.¹⁶ In short, [¹⁸F]FLT serves as an excellent imaging agent for the diagnosis of cancers associated with breast, lung, brain, etc. However, precursors for [¹⁸F]FLT, 4/5a/5b (Fig. 1), are quite expensive for deployment in routine clinical practice. In order to address this concern, herein we report in-house

synthesis of [¹⁸F]FLT precursors, 4/5a/5b (Fig. 1) in an economical way, from easily available starting material thymidine. With the implementation of effective [¹⁸F] labelling techniques²³⁻²⁷, it is now possible to formulate [¹⁸F]FLT from these precursors to cater to the national demand.

Results and Discussion

Among the three known precursors (4/5a/5b) (Figure 1), we initially targeted the synthesis of nosyl compound 4, as it is the most commonly used precursor to generate [¹⁸F]FLT by radiolabelling using ¹⁸F. The complexity associated with the synthesis of precursor 4 is well documented in literature.²⁸ Therefore care was taken while designing the synthetic path and reaction conditions to achieve the target. Thus, as shown in Scheme 1, C5 hydroxy group (C5(OH)) in thymidine 1 was initially protected using an acid labile protecting group, dimethoxy trityl chloride (DMTrCl), in pyridine, with DMAP as activator, to afford dimethoxy trityl protected thymidine 7 in 75% yield. The C5 protected thymidine 7 was subjected to mesylation using mesylchloride and triethyl amine (TEA) to yield corresponding mesylated product, which, without isolation, was heated for 2 h to afford a bicyclic intermediate, through intramolecular nucleophilic substitution. This reaction mixture was subjected to in situ hydrolysis using ethanolic sodium hydroxide under reflux to furnish C3 inverted dimethoxy trityl protected thymidine 8. This one pot three step process yielded the inverted alcohol at C3-position in 78% yield. The next step was to convert the C3(OH) in (6) to a leaving group, nosylate.

Thus, as an initial attempt, compound 8 was treated with nosylchloride (NsCl) in pyridine. However, to our surprise, this reaction condition did



Scheme 1: Synthesis of [¹⁸F]FLT precursor (4)

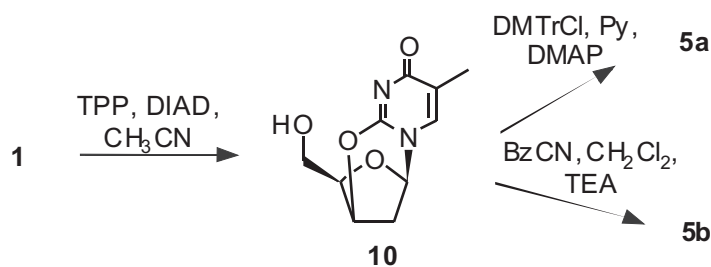
not produce any desired product. But the same reaction when performed in the presence of silver-O-triflate yielded the nosylated adduct (9) as a slight yellow foamy solid in 63% yield. Final step in the synthesis of precursor 4 was to mask secondary amine functionality present in the thymine group. To realize it, nosylate 9 was reacted with Boc-anhydride in pyridine to afford the targeted [¹⁸F]FLT precursor 4 with an overall yield of 7%. Analytical data, HRMS, ¹H and ¹³C NMR studies confirmed the structural integrity of the compound 4.^{29,30}

Purity of the synthesized material was further established by HPLC analysis wherein in-house made precursor 4 eluted at same retention time to that of commercially available material. The HPLC profile and MS data of the in-house made precursor is shown in Fig. 2 (A).

Extensive review of available literature, revealed that, radiolabelling of nosyl derivative 4 would yield [¹⁸F]FLT with a radiochemical yield of ~50%.²⁹ This relatively less radiochemical yield, is partially due to moderate labelling with ¹⁸F and partly

owing to the formation of elimination product, Stavudine (antiretroviral drug, d4T) 6, side products like furfuralic alcohol, chlorothymidine, fluorinated nosyl derivatives,^{31,32} etc arising due to the decomposition/incomplete reaction of the precursor. The formation of these side products³³ automatically enforces an additional HPLC purification step on the labelled material before its administration to patients. This not only results in loss of radioactivity but also consumes valuable time that could otherwise be utilised for its transportation to destined hospitals. Alternatively, anhydro derivatives of thymidine, namely 5'-O-(4,4'-Dimethoxytrityl)-2,3'-anhydrothymidine 5a and 5'-O-

(benzoyl)-2,3'-anhydrothymidine 5b, are also known to produce the desired labelled product 3 and can be used without complex purification steps. Even though 5a/b are less expensive than 4, the radiochemical yield of [¹⁸F]FLT derived from 5a/b is not more than 16%.²⁹ A close look at the chemical structure of precursors 5a/b showed that they constitute two protecting group variants at C5(OH) of anhydro derivative 10, wherein the protecting group of C5(OH) in 5a is acid labile and that in 5b is base labile. These precursors would provide the much-needed flexibility to synthesize [¹⁸F]FLT, devoid of any side-products, employing appropriate radiolabelling-deprotection protocols.



Scheme 2: Synthesis of [¹⁸F]FLT precursor (5a) and (5b)

For the synthesis of precursors 5a and 5b, a synthetic sequence as portrayed in scheme 2 was pursued. Reminiscent to the synthesis of 4, thymidine 1 was used as the starting material for the synthesis of precursors 5a/b. Thus reaction of 1 under Mitsunobu condition,³⁴ i.e. triphenyl phosphine and diisopropylazodicarboxylate (DIAD) in acetonitrile, afforded the anhydro compound 10 in 80% yield.^{35,36} To accomplish the synthesis of acid labile precursor 3b, C5(OH) in anhydro compound 10 was reacted with DMTrCl in pyridine to afford DMTr protected anhydro derivative 5a in ~85% yield. On the other hand to accomplish the synthesis of base labile

precursor 5b, substrate 10 was reacted with benzoyl cyanide in the presence of TEA.

The desired benzoate adduct 5b was obtained in ~89% yield. The structure of 5a/b was confirmed by NMR, and MS analysis.^{37,38} The HPLC profile, mass spectra and the physical appearance (D) of the synthesized precursors 4/5a/5b, (A,B,C) are shown in figure 2.

EXPERIMENTS & METHODS

The IR spectra were recorded as a thin film (liquids) with a Shimadzu FTIR-8400 spectrometer. The ¹H (500 MHz) and ¹³C (125 MHz) NMR spectra were

recorded with a Varian instrument in CD₃CN/CD₂Cl₂/CDCl₃/DMSO-D₆. MS was recorded on Advion Mass Spectrometer. Thin layer chromatography was performed on pre-coated plates (0.25 mm, silica gel 60 F254), and the spots were visualized by UV light or spraying with 3.5% solution of 2,4-dinitrophenylhydrazine in ethanol/H₂SO₄ or with basic aqueous KMnO₄ solution followed by heating. All the materials used for the synthesis was purchased from Sigma-Aldrich. HPLC was recorded using BetaSil™ Silica HPLC Columns (5μm, 4.6 mm x 150 mm), with acetonitrile as mobile phase over 25 min.

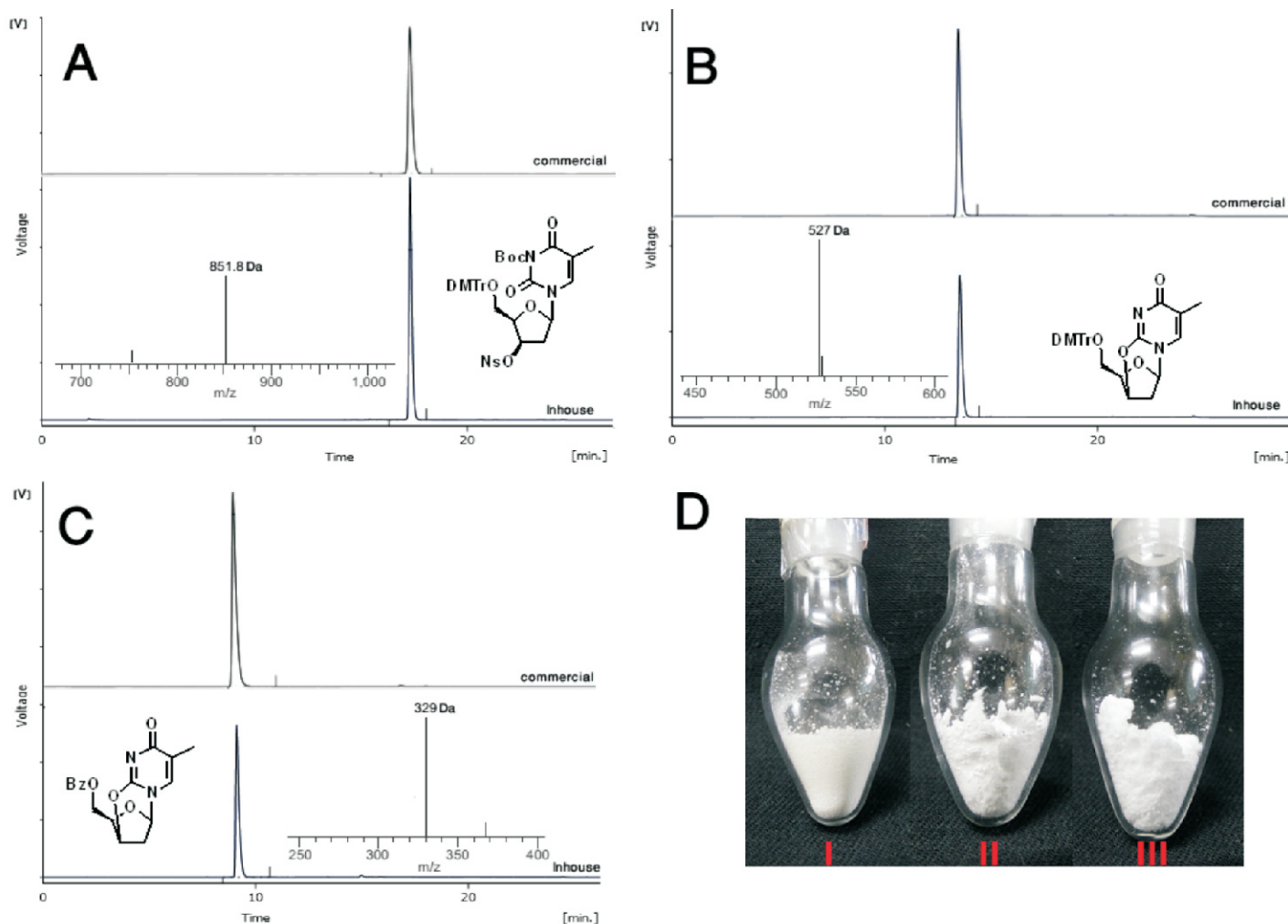


Fig. 2: HPLC trace and photographic images of indigenously developed [¹⁸F]FLT precursors: (A) Precursor 4, (B) Precursor 5a, (C) Precursor 5b and (D) Photographic images of 4 (I), 5a (II), and 5b (III)

| [5-O-(4,4-Dimethoxytriphenylmethyl)-2-deoxy-D-erythropentofuranosyl]thymine(7) | [5-O-(4,4-Dimethoxytriphenylmethyl)-2-deoxy-D-threopentofuranosyl]thymine(8) | 1-(2-deoxy-3-O-(4-nitrobenzenesulfonyl)-5-O-(4,4*-dimethoxy-trityl)-β-D-threo-pentofuranosyl)-thymine(9) |
|---|---|---|
| <p>A solution of thymidine (1.50 g, 6.19 mmol) and dimethoxytrityl chloride (2.54 g, 7.49 mmol) in pyridine (20 mL) was stirred for 3 h at room temperature. After completion of reaction (tlc) it was neutralized with acetic acid and concentrated under vacuum. The residue was purified by column chromatography on silica gel with n-hexane:ethyl acetate (1:3, v/v) to give (7) as a brown foamy solid (2.52g, 75%); R_f 0.48 (100% ethyl acetate); mp 114.0–116.0°C (sublimation) (lit.114.0–116.0°C (sublimation));³⁰ IR (neat): ν_{max} 2929, 1674, 1606, 1506, 1247, 1031 cm⁻¹; ¹H NMR (500 MHz, CD₃CN) δ 9.71 (s, 1H, exchangeable with D₂O), 7.64 (s, 1H), 7.51 (d, J = 7.6 Hz, 2H), 7.42 – 7.29 (m, 6H), 7.27 – 7.22 (m, 1H), 6.89 (d, J = 7.4 Hz, 4H), 6.18 – 6.12 (m, 1H), 4.31 (s, 1H), 4.11 (dd, J = 7.0, 3.4 Hz, 1H), 3.77 (s, 6H), 3.48 (dd, J = 10.1, 7.6 Hz, 1H), 3.34 (dd, J = 10.3, 3.4 Hz, 1H), 2.64 – 2.53 (m, 1H), 2.41 (bs, 2H, one proton exchangeable with D₂O), 1.73 (s, 3H); ¹³C NMR (125 MHz, CD₃CN) δ 164.3, 158.7, 150.9, 145.2, 137.5, 136.0, 135.9, 130.0, 129.1, 128.1, 127.9, 127.7, 126.9, 117.4, 109.3, 86.2, 85.1, 83.5, 70.0, 62.8, 54.9, 40.7, 11.8.</p> | <p>To an ice cooled solution of (7) (2.50 g, 4.66 mmol) in CH₂Cl₂ (30 mL) was added methanesulfonyl chloride (1.16 ml, 15.00 mmol), and triethyl amine (3.25 mL, 23.30 mmol). After 3 h, the reaction mixture was diluted with CH₂Cl₂ (75 mL) washed with saturated NaHCO₃ solution (20 mL x 2) and H₂O (20 mL x 2). The organic phase was dried over anhydrous Na₂SO₄, concentrated and dissolved in EtOH (120 mL) and 3 mL of 10 N NaOH solution was added. After the solution was heated for 1.5 h at 80°C, it was neutralized with acetic acid and concentrated under vacuum. The residue was extracted using CH₂Cl₂ (75 mL) and purified by column chromatography on silica gel (hexane/ethyl acetate = 20/80, v/v) to yield (8) as a light brown foamy solid (1.97 g, 78%); R_f 0.48 (100% ethyl acetate); mp 134.0–137.0°C (sublimation); IR (neat): ν_{max} 2939, 1681, 1613, 1508, 1247, 1176 cm⁻¹; ¹H NMR (500 MHz, CD₃CN) δ 9.71 (s, 1H, exchangeable with D₂O), 7.64 (s, 1H), 7.49 (t, J = 9.4 Hz, 2H), 7.42 – 7.21 (m, 7H), 6.89 (m, 4H), 6.18 – 6.06 (m, 1H), 4.36 – 4.27 (m, 1H), 4.10 (m, 1H), 3.78 (s, 6H), 3.49 – 3.39 (m, 1H), 3.36 – 3.28 (m, 1H), 2.59 (m, 1H), 2.41 (bs, 2H, one proton exchangeable with D₂O) 1.73 (d, J = 0.5 Hz, 3H); ¹³C NMR (125 MHz, CD₃CN) δ 163.9, 158.7, 150.7, 145.2, 137.4, 136.0, 135.9, 130.0, 128.0, 127.9, 126.8, 117.4, 109.2, 86.2, 85.0, 83.4, 69.9, 62.8, 54.9, 40.6, 11.8.</p> | <p>4-Nitrobenzenesulfonyl chloride (1.58 g, 7.16 mmol) and silver-O-triflate (1.84 g, 7.16 mmol) was added to a stirred solution of (8) (1.95 g, 3.58 mmol) in pyridine (25 mL) at 0 °C. After 30 min, the cooling bath was removed, and the solution was stirred at room temperature until reaction shows complete conversion (tlc). Subsequently, the reaction mixture was diluted with 25 mL of water and extracted with chloroform (3×50 mL). The combined organic layers post washing with saturated KHCO₃ (50 mL) and water (20 mL) was dried with magnesium sulfate and evaporated to dryness under reduced pressure. The residue was purified by column chromatography (ethyl acetate/hexane=40/60, v/v) to yield (9) 1.65 g, 63%; R_f 0.35; 60% ethyl acetate-hexane); mp 87-94 °C (Lit. 85.9–93.4 °C);³⁰ IR (neat): ν_{max} 2929, 1681, 1606, 1506, 1176, 900 cm⁻¹; ¹H NMR (500 MHz, CD₂Cl₂) δ 10.15 (s, 1H, exchangeable with D₂O), 8.28 (d, J = 8.8 Hz, 2H), 7.93 (d, J = 8.8 Hz, 2H), 7.44 (d, J = 7.7 Hz, 2H), 7.34 – 7.22 (m, 8H), 6.88 (d, J = 8.6 Hz, 4H), 6.24 (dd, J = 7.6, 2.9 Hz, 1H), 5.26 (m, 1H), 4.28 (dd, J = 9.2, 5.3 Hz, 1H), 3.83 (s, 6H), 3.57 (dd, J = 10.2, 6.5 Hz, 1H), 3.25 (dd, J = 10.2, 4.8 Hz, 1H), 2.82 (m, 1H), 2.46 (dd, J = 15.9, 2.5 Hz, 1H), 1.78 (s, 3H); ¹³C NMR (125 MHz, CD₂Cl₂) δ 164.2, 158.8, 158.8, 150.9, 150.7, 144.5, 141.5, 135.5, 135.3, 135.0, 130.0, 130.0, 129.0, 128.1, 128.0, 127.9, 127.0, 124.6, 113.2, 113.1, 110.7, 86.8, 84.2, 81.7, 80.6, 61.5, 55.2, 39.3, 12.2.</p> |

| 3-N-Boc-1-[5-O-(4,4-dimethoxytrityl)-3-O-nosyl-2-deoxy-lyxofuranosyl]thymine(4) | O ² ,O ³ -anhydro-1-(2-deoxy-β-D-threo-pentofuranosyl)thymine(10) | 5'-O-(4,4'-Dimethoxytrityl)-2,3'-anhydrothymidine(5a) |
|---|--|--|
| <p>4,4'-Dimethylminopyridine (0.24 g, 1.95 mmol) in THF (4 mL) and di-tert-butylidicarbonate (0.47 g, 2.14 mmol) were added to a solution of compound (9) (1.30 g, 1.78 mmol) in THF (4 mL) at 25 °C with stirring. After 2 h of stirring, the solvent was removed in vacuo, and the residue was purified by silica gel flash column chromatography using MeOH/CH₂Cl₂ (5/95, v/v) as eluent to give the 3-tert-butoxycarbonyl product (4) as a foamy solid (1.10 g, 75 %); R_f 0.48; (35% ethyl acetate-hexane); mp 119-121 °C (Lit. 118.8–120.6 °C);³⁰ IR (neat): ν_{max} 2941, 1782, 1712, 1658, 1249, 1178, 904 cm⁻¹; ¹H NMR (500 MHz, CD₃CN) δ 8.34 – 8.25 (m, 2H), 7.98 – 7.89 (m, 2H), 7.45 – 7.39 (m, 2H), 7.36 – 7.23 (m, 8H), 6.89 (d, J = 8.3 Hz, 4H), 6.11 (dd, J = 7.6, 2.5 Hz, 1H), 5.30 (t, J = 3.9 Hz, 1H), 4.40 – 4.28 (m, 1H), 3.80 (d, J = 2.0 Hz, 6H), 3.40 (dd, J = 10.3, 6.9 Hz, 1H), 3.16 (dd, J = 10.3, 4.3 Hz, 1H), 2.80 (ddd, J = 15.9, 7.6, 5.1 Hz, 1H), 2.36 (dd, J = 16.0, 1.6 Hz, 1H), 1.68 (d, J = 1.0 Hz, 3H), 1.58 (s, 9H); ¹³C NMR (125 MHz, CD₃CN) δ 162.1, 159.9, 152.1, 149.4, 149.3, 145.8, 142.3, 136.7, 136.6, 136.0, 131.1, 130.0, 129.0, 128.0, 125.9, 118.3, 114.3, 114.2, 110.5, 87.6, 87.4, 86.0, 82.9, 82.2, 62.7, 56.0, 40.0, 27.7, 12.8.</p> | <p>To a solution of thymine (1) (3.00 g, 12.38 mmol) and triphenyl phosphine (6.49 g, 24.77 mmol) in CH₃CN (24 mL) was added diisopropylazodicarboxylate (4.86 mL, 24.77 mmol). After completion of reaction on tlc, reaction mixture was cooled to -20 °C and was poured to chilled ethyl acetate solution to precipitate out the desired lactone (10) in 80% yield (2.21 g). R_f 0.30; 15% MeOH - CH₂Cl₂; mp 230–231 °C; (lit. 230–231 °C);^{14,35} IR (neat): ν_{max} 3315, 1660, 1625, 1531, 1479, 1136 cm⁻¹; ¹H NMR (500 MHz, DMSO-D6) δ 7.55 (s, 1H), 5.80 (s, 1H), 5.23 (s, 1H), 5.06 (s, 1H), 4.18 (s, 1H), 3.47 (d, J = 5.8 Hz, 2H), 2.49 (m, 2H), 1.74 (s, 3H); ¹³C NMR (125 MHz, DMSO-D6) δ 171.4, 154.1, 137.2, 116.4, 87.2, 85.7, 77.3, 60.1, 33.1, 13.4.</p> | <p>To a solution of lactone (10) (1.00 g, 4.47 mmol) in pyridine (20 mL) was added DMTrCl (1.83 g, 5.37 mmol). After completion of reaction on tlc, reaction mixture was concentrated and purified using silica gel column chromatography with MeOH/CH₂Cl₂ (10/90, v/v) to yield (5a) in 85% yield (1.99 g); R_f 0.30; (5% MeOH - CH₂Cl₂); mp 114-116 °C (subl.) (Lit. mp 114-116 °C (sublimation));^{39,40} IR (neat): ν_{max} 1663, 1620, 1504, 1463, 1134 cm⁻¹; ¹H NMR (500 MHz, CD₃CN) δ 7.54 – 7.40 (m, 2H), 7.36 – 7.18 (m, 8H), 6.95 – 6.79 (m, 4H), 5.64 (d, J = 3.8 Hz, 1H), 5.20 (s, 1H), 4.41 (td, J = 6.4, 2.5 Hz, 1H), 3.78 (s, 6H), 3.21 (d, J = 6.4 Hz, 2H), 2.63 – 2.50 (m, 1H), 2.51 – 2.38 (m, 1H), 1.85 (d, J = 1.1 Hz, 3H); ¹³C NMR (125 MHz, DMSO-D6) δ 170.8, 158.1, 158.1, 153.5, 144.6, 136.8, 135.3, 135.1, 129.7, 127.9, 127.6, 126.7, 116.2, 113.2, 86.9, 85.8, 83.6, 77.2, 62.3, 55.1, 32.8, 13.0.</p> |

5'-O-Benzoyl-2,3'-anhydrothymidine(5b)

To a solution of lactone (10) (1.00 g, 4.47 mmol) in CH₂Cl₂ (20 mL) was added benzoyl cyanide (0.71 g, 5.37 mmol). After completion of reaction on tlc, reaction mixture was concentrated and purified using silica gel column chromatography with MeOH/CH₂Cl₂ (10/90, v/v) to yield (5b) in 89% yield (1.30 g); R_f 0.40; (15% MeOH - CH₂Cl₂); mp 237–242 °C (lit. 241 °C);³⁶ IR (neat): ν_{max} 1656, 1622, 1556, 1479, 1134, 1070 cm⁻¹; ¹H NMR (500 MHz, CD₃CN) δ 7.97 (dd, J = 8.3, 1.1 Hz, 2H), 7.68 – 7.60 (m, 1H), 7.49 (td, J = 7.6, 1.7 Hz, 2H), 7.22 (d, J = 1.2 Hz, 1H), 5.67 (d, J = 3.9 Hz, 1H), 5.33 (s, 1H), 4.66 – 4.53 (m, 2H), 4.51 – 4.41 (m, 1H), 2.60 (dd, J = 13.1, 1.3 Hz, 1H), 2.53 (ddd, J = 13.1, 3.9, 2.8 Hz, 1H), 1.82 (d, J = 1.2 Hz, 3H); ¹³C NMR (125 MHz, DMSO-D₆) δ 172.9, 166.6, 154.6, 138.0, 134.5, 130.0, 129.6, 129.5, 117.4, 88.1, 82.8, 78.5, 62.8, 33.6, 13.6.

Conclusion

Three [¹⁸F] FLT precursors were synthesized from commercially available thymidine in a highly economical manner. Their characterisation using various techniques such as HPLC, NMR and MS confirmed the molecule's structural integrity and purity. With the latest success, we are strongly positioned to synthesise these precursors in gram quantities with high purity and also make them available to hospitals at below 1/10th of the market price. The precursor 4 was successfully labelled with ¹⁸F whereas radiopharmaceutical preparation of precursor 5a/5b would be completed in due course of time.

Acknowledgments

KSAK is thankful to Prof S. K. Nayak, and Prof S. Chattopadhyay, former Head, BOD, and Group Director, Bio Science Group, BARC for their encouragement and support throughout the course of this activity.

***Corresponding author**

Dr. K. S. Ajish Kumar

References

- Hargreaves, R. J. and Rabiner, E. A. Neuro. Boil. Dis. 2014, 61, 32-38.
- Saint-Aubert, L., Lemoine, L., Chiotis, K., Leuzy, A., Rodriguez-Vieitez, E. and Nordberg, A. Mol. Neurodegen. 2017, 12, 1-21.
- Jacobson, O. and Chen, X. Curr. Top. Med. Chem. 2010, 10, 1048-1059.
- Mankoff, D. A., Shields, A. F. and Krohn K. A. Radiol. Clin. N. Am. 2005, 43, 153 – 167.
- Vallabhajosula, S., Solnes, L. and Vallabhajosula, B. Sem. Nucl. Med. 2011, 41, 246-264.
- Kornberg A. Biosynthesis of DNA precursors. In: DNA Replication, 2nd ed., (Edited by Kornberg A. and Baker T.), 1992, pp 53–100, W. H. Freeman and Co., New York.
- Christman D., Crawford E. J., Friedkin M. and Wolf A. P. Proc. Natl. Acad. Sci. USA 1972, 69, 988–992.
- Eary J. F., Mankoff D. A., Spence A. M., Berger M. S., Olshen A., Link J. M., O'Sullivan F. and Krohn K. A. Cancer Res. 1999, 59, 615–621.
- Mankoff D. A., Shields A. F., Link J. M., Graham M. M., Muzi M., Peterson L. M., Eary J. F. and Krohn K. A. J. Nucl. Med. 1999, 40, 614–624.
- Mankoff D. A., Shields A. F.,

- Graham M. M., Link J. M., Eary J. F. and Krohn K. A. J. Nucl. Med. 1998, 39, 1043–1055.
- Shields A. F., Lim K., Grierson J. R., Link J. M. and Krohn K. A. J. Nucl. Med. 1990, 31, 337–342.
- Grierson J. R. and Shields A. F., Krohn K. A. Nucl. Med. Biol. 2000, 27, 143-156 and references cited therein.
- Herdewijn P., Balzarini J., De Clercq E., Pauwels R., Baba M., Broder S. and Vanderhaeghe H. J. Med. Chem. 1987, 130, 1270–1278.
- Balogopala, M. I., Ollapally A. P. and Lee H. J. Nucleos. Nucleot. 1996, 15, 899–906.
- Sigmund H. and Pfeleiderer W. Helv. Chim. Acta. 1996, 79, 426-438.
- Shields A. F., Grierson J. R., Dohmen B. M., Machulla H. J., Stayanoff J. C., Lawhorn-Crews J. M., Obradovich J. E., Muzik O. and Mangner T. J. Nat. Med. 1998, 4, 1334–1336.
- Grierson J. R. and Shields A. F. J. Labelled Compd. Radiopharm. 1999, 42, S525–S526.
- Arn'er E. S., Spasokoukotskaja T. and Eriksson S. Biochem. Biophys. Res. Commun. 1992, 188, 712–718.
- Sherley J. L. and Kelly T. J. J. Biol. Chem. 1988, 263, 8350–8358.
- Matthes E., Lehmann C., Scholz D., Rosenthal H.-A. and Langen P. Biochem. Biophys. Res. Commun. 1988, 153, 825–831.
- Langen P., Etzold G., Hintsche R. and Kowollick G. Acta. Biol. Med. Ger. 1969, 23, 759–766.
- Nakajo M., Jinguji M., Fukukura Y., Nakajo M., Kajiya Y. and Tani A. J. Nucl. Med. 2014, 55, S1, 1925.

23. Javed M. R., Chen S., Kim H-K., Wei L., Czernin J., Kim Chang-Jin "CJ", Dam R. M.-van and Keng P., Y. J. Nucl. Med. 2013, 55, 321-328.
24. Collins J., Waldmann C. M., Drake C., Slavik R., Ha N. S., Sergeev M., Lazari M., Shen B., Chin F. T., Moore M., Sadeghi S., Phelps, M. E., Murphy J. M. and Dam R. M. van. Proc. Natl. Acad. Sci. USA. 2017, 114, 11309-11314.
25. Marchand P., Ouadi A., Pelliccioli M., Schuler J., Laquerriere P., Boisson F. and Brasse D. Nucl. Med. and Biol. 2016, 43, 520-527.
26. Tang G., Tang X., Wen F., Wang M., Li B. Appl. Rad. and Iso. 2010, 68, 1734-1739.
27. Kim D. W., Ahn D-S., Oh Y-Ho., Lee S., Kil H. S., Oh S. J., Lee S. J., Kim J. S., Ryu J. S., Moon D. H. and Chi D. Y. J. Am. Chem. Soc. 2006, 128, 16394-16397.
28. Velangupurackel W. Synthetic routes to the tumor proliferation biomarker FLT and ProTide analogues for PET imaging, 2014, Ph.D thesis, Cardiff University.
29. Yun M., Oh S. J., Ha H. J., Ryu J. S. and Moon D. H. Nucl. Med. Biol. 2003, 30, 151-157.
30. Martin S. J., Eisenbarth J. A., Wagner-Utermann U., Mier W., Henze M., Pritzkow H., Haberkorn U. and Eisenhut M. Nucl. Med. Biol. 2002, 29, 263-273.
31. Nandy S. K. Krishnamurthy N. V. and Rajan M. G. R. J. Radioanal. Nucl. Chem. 2010, 283, 245-251.
32. Pascali C., Bogni A., Fugazza L., Cucchi C., Crispu O., Laera L., Iwata R., Maiocchi G., Crippa F., and Bombardieri E. J. Radioanal. Nucl. Chem. 2012, 39, 540-550.
33. Marchand P., Ouadi, A., Pelliccioli M., Schuler J., Laquerriere P., Boisson F. and Brasse D. Nucl. Med. and Biol. 2016, 43, 520-527.
34. Mitsunobu O. Synthesis, 1981, 1-26.
35. Fox J. J. and Miller N. C. J. Org. Chem. 1963, 28, 936-941.
36. Czernecki S., and Valery J-M. J. Chem. Soc., Chem. Commun. 1990, 801-802.
37. Blocher A., Ehrlichmann W., Kuntzsch M., Wei R., Grierson J. R. and Machulla H. J. J. Nucl. Med. 2000, 41:147P [Suppl.].
38. Blocher A., Bieg C., Ehrlichmann W., Dohmen B. M. and Machulla H. J. J. Nucl. Med. 2001, 42:257P [Suppl.].
39. Blocher A., Kuntzsch M., Wei R., and Machulla H.-J. J. Radioanal. and Nucl. Chem. 2002, 251, 55-58.
40. Machulla H. J. Blocher A., Kuntzsch M., Piert M., Wei R., Grierson J. R. J. Radioanal. Nucl. Chem. 2000, 243, 843-846.

Development of Eco-friendly Biopesticide Formulation for Mosquito Larvae Control

Ashok B. Hadapad, Arpit Prashar, Vikas, Ramesh S. Hire*

Nuclear Agriculture & Biotechnology Division

Omkar Kinkar, Ravindra D. Makde

Beamline Development and Application Section, Physics Group

Abstract

Mosquito species of *Anopheles*, *Aedes* and *Culex* are major vectors for malaria, dengue, zika, chikungunya, filariasis and Japanese encephalitis diseases. *Bacillus thuringiensis subsp. israelensis (Bti)* is spore-forming bacterium having worldwide distribution produces proteins which are toxic to these mosquito larvae. The local isolate, *Bti* ISPC-12 showed high toxicity to mosquito larvae of *Anopheles stephensi*, *Aedes aegypti* and *Culex quinquefasciatus*. The genes encoding insecticidal toxin proteins have been expressed in the *E. coli* expression system for molecular and structural studies. Sustained-release formulation using spore-crystal powder of *Bti* ISPC-12 has been developed. The spore-crystal powder (active ingredient) and formulation has been found to be safe to mammals. Field studies carried out in Anushaktinagar, Mumbai and RRCAT, Indore townships demonstrated the efficacy against mosquito larvae. Thus *Bti* ISPC-12 based formulation is a potent biopesticide for the management of mosquito population.

Keywords: Biopesticide, *Bti* ISPC-12, Cry proteins, field study, integrated vector management, mosquitoes

Introduction

Mosquitoes are one of the important insect vectors responsible for transmitting malaria, filariasis, dengue, Japanese encephalitis, West Nile fever and more recently Zika diseases. These diseases are transmitted by many species of *Anopheles*, *Aedes* and *Culex* genera (Diptera: Culicidae). Several strategies are being employed to annihilate the mosquito population in order to minimise the vector-borne disease transmission. Chemical and biological control agents remain important components of mosquito-vector control. However, chemical approach has resulted negative impact on the ecosystem and human health, and faster development of resistance to insecticide [1,2].

B. thuringiensis subsp. israelensis (Bti) is an aerobic, gram-positive, endospore forming entomopathogenic bacterium commonly found in soil, water, dead insects and phyloplanes and was first isolated in 1976 at Negev

desert in Israel [3]. So far, *Bti* is the most effective microbial control agent for mosquito and blackfly [4,5]. This bacterium is known to produce intracellular crystal inclusions during sporulation. The crystal inclusions are composed of multiple protein components of 134 kilodalton (kDa), 128 kDa, 72 kDa, 27 kDa, 78 kDa and 29 kDa encoded by *cry4Aa*, *cry4Ba*, *cry11Aa*, *cyt1Aa*, *cry10Aa* and *cyt2Ba* genes, respectively [6,7]. The insecticidal activity is attributed to the presence of these proteins. These insecticidal toxins also called as δ -endotoxins or Cry toxins, are highly specific to mosquitoes due to presence of specific receptors and thus have no adverse effects on non-target invertebrates and vertebrates [8,9]. In addition, the advantage of *Bti* as biocontrol agent over all other larvicides is that it has low probability of developing resistance in mosquito larvae due to presence of multiple toxins [7,10]. Various formulations based on *Bti* have been registered and in use worldwide for mosquito larvae control [4]. However, the success of

using *Bti* as an effective biopesticide under field conditions mainly depends upon the development of suitable formulations.

In Nuclear Agriculture & Biotechnology Division (NA&BTD), our section has isolated and identified several entomopathogens from samples collected from insect mass rearing facility, drainages and fields [11,12]. These entomopathogens have been extensively tested for the insecticidal activity against agriculturally important insect pests and mosquito larvae of different genera. Among these, *Bti* isolate ISPC-12 is very effective against *Aedes aegypti*, *Anopheles stephensi* and *Culex quinquefasciatus*.

Bacterial isolate, mosquito cultures and laboratory assays

Bti ISPC-12 was isolated from dead *Ae. aegypti* mosquito larvae collected from drainages of Trombay village, Mumbai. The bacterial culture was maintained on standard nutrient agar (NA) supplemented with 0.3%

molasses. The grown bacterial culture (24 h) comprising spore-crystal mixture was lyophilized and stored at 4°C for further studies.

The mosquito cultures of *A. stephensi*, *Ae. aegypti* and *C. quinquefasciatus* were maintained in insect mass rearing facility at NA&BTD, BARC, Mumbai [13]. The mosquito larvicidal activity of spore-crystal mixtures (~1 x 10⁵ spores/mL) of *Bti* ISPC-12 along with control (without *Bti* spore-crystal mixture) were tested against third-instar larvae of mosquitoes [12]. The results indicated >98% mortality of *A. stephensi*, *Ae. aegypti* and *C. quinquefasciatus* within 24 h (Fig. 1). The higher toxicity to mosquito larvae may be due to presence of multiple insecticidal toxins in *Bti* ISPC-12 isolate.

Characterisation of mosquito-larvicidal toxins

The genes encoding insecticidal toxin proteins in *Bti* ISPC-12 and standard *Bti* strain 4Q2-72 was studied. The presence of four major polypeptides ~134, 128, 72 and 27 kDa encoded by *cry4Aa*, *cry4Ba*, *cry11Aa*, *cyt1Aa* genes and two minor polypeptides 78 and 29 kDa encoded by *cry10Aa* and *cyt2Ba* genes in *Bti* ISPC-12 has been confirmed by PCR and subsequent DNA sequencing. Further, PCR products were cloned into *E. coli* expression plasmid pST50Tr [14] and the integrity of the genes were confirmed by DNA sequencing. These δ-endotoxins form a complex parasporal crystalline body with remarkably high and specific toxicity to *Aedes*, *Anopheles* and *Culex* larvae [7].

The crystals (containing δ-endotoxins) were purified from spore-crystal powder of *Bti* ISPC-12 using sucrose-density gradient centrifugation as shown in Fig. 2 and three major polypeptides were observed comprising Cry4Aa (130 kDa), Cry11Aa (72 kDa) and

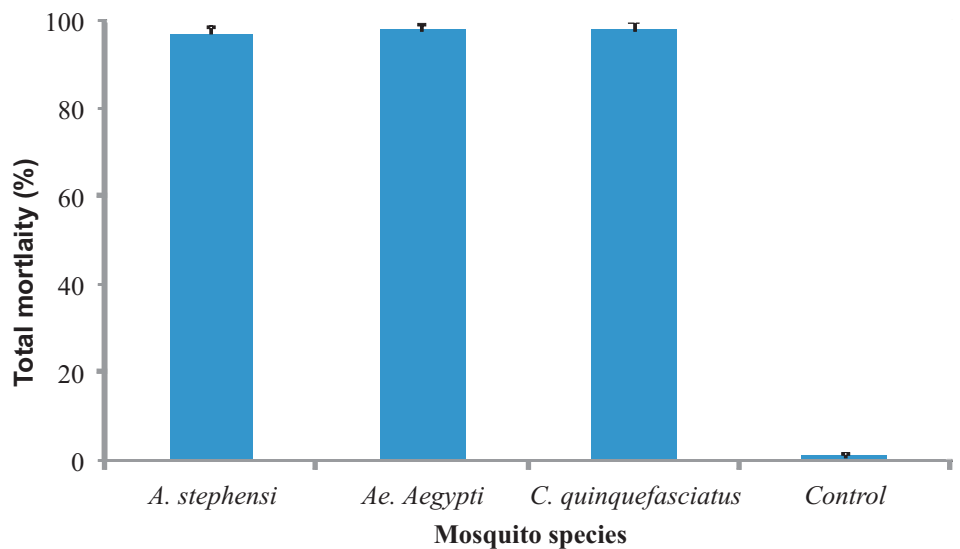


Fig. 1: Larvicidal activity of *Bacillus thuringiensis* subsp. *israelensis* strain ISPC-12 against third-instar larvae of different mosquito species. Error bars indicates mean ± standard error (SE) of four replications.

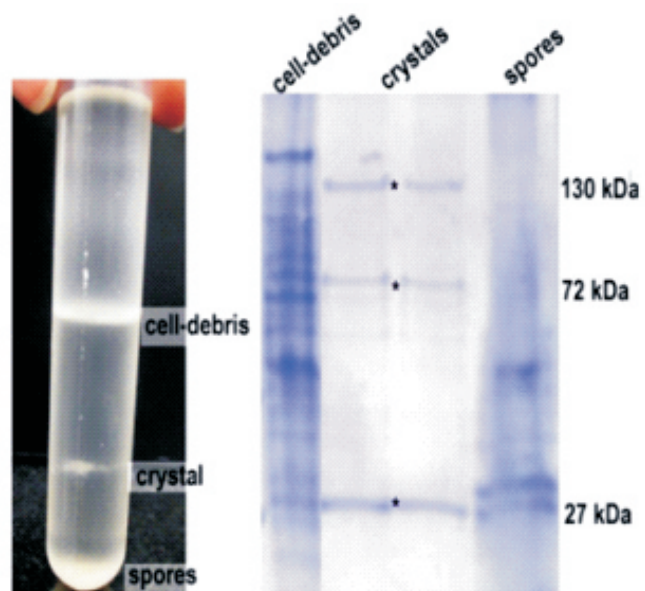


Fig. 2: Different mosquito larvicidal proteins in *Bti* ISPC-12. Purification of native crystal toxins using density gradient ultra-centrifugation. Left panel shows the separation of toxin crystals in sucrose density gradient of 67 to 79 %. The right panel shows three different toxin proteins (kilodalton; kDa) bands in lanes 2 and 3 crystals

Cyt1Aa (27 kDa). The higher toxicity of this strain may be due to the presence of these polypeptides in large quantity.

Development of biopesticide formulation

The sustained-release biopesticide formulation comprising biopolymer,

active ingredient (spore-crystal powder of *Bti* ISPC-12) and floating agent was prepared [15]. This formulation is effective against mosquito larvae (Fig. 3A and B). The formulation is mild yellow in colour (Fig. 3C), odourless and the granule size of the formulation was typically in the range of 1-2 mm. The developed

formulation is effective against different genera of mosquito larvae under laboratory conditions (Fig. 3D).

Toxicological studies on non-target organisms

The active ingredient (AI) and formulation should not have adverse effects on mammals and other beneficial organisms. This is the prerequisite for obtaining registration from Central Insecticide Board & Registration Committee (CIB&RC) for manufacturing and commercialisation in India. Hence, the toxicity of AI and formulation of *Bti* ISPC-12 was carried out by CIB recognised laboratory using Organization for Economic Cooperation and Development (OECD) and Good Laboratory Practices (GLP) guidelines. The extensive study using AI and formulation concluded that neither *Bti* ISPC-12 spore-crystal mixture (AI) nor the formulation based on it is toxic to mammals (Rats, Guinea pigs and Rabbits) and other beneficial organisms thereby confirming that the *Bti* ISPC-12 biopesticide is safe for humans and environment.

Small-scale field evaluation

The bioefficacy of biopesticide formulation based on *Bti* ISPC-12 was tested in small-scale field experiments as per WHO guidelines [16]. Different doses of biopesticide formulation were tested in plastic tubs (5 L capacity) (Fig. 4A) and water tank with metallic mesh lid (200 L capacity) (Fig. 4C). Mosquito larvae of *Ae. aegypti* and *C. quinquefasciatus* were added and allowed to acclimatise for 4 h before biopesticide formulation treatment. The observations were recorded after 24 h along with control and mortality was corrected with Abbott formula [17]. The results indicated that $98.53 \pm 0.45\%$ and $98.82 \pm 0.33\%$ total mortality was recorded in *Ae. aegypti* and *C. quinquefasciatus* larvae in tub

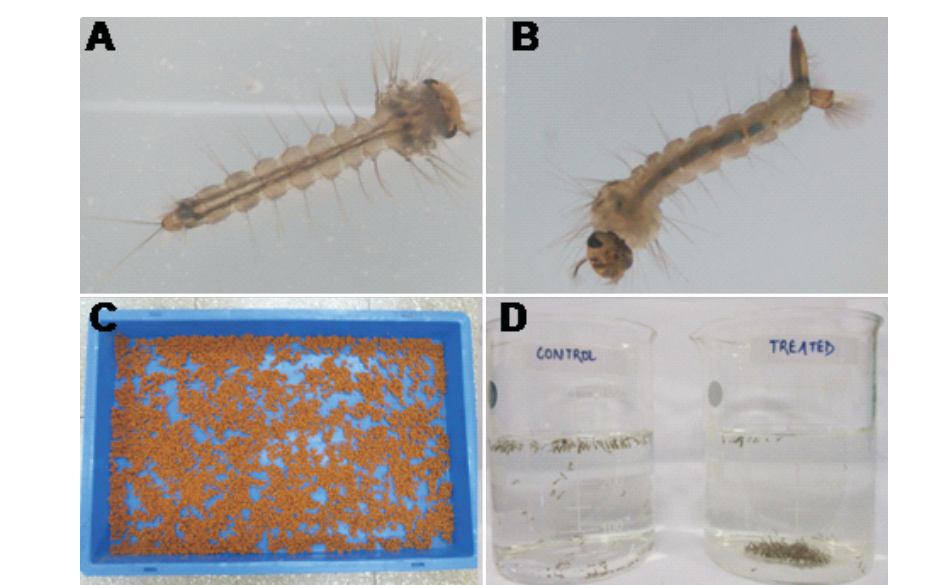


Fig. 3: Development and testing of biopesticide formulation based on *Bacillus thuringiensis* subsp. *israelensis* strain ISPC-12. A & B. Mosquito larvae; C. Biopesticide formulation; D. Bioefficacy of formulation under laboratory conditions.

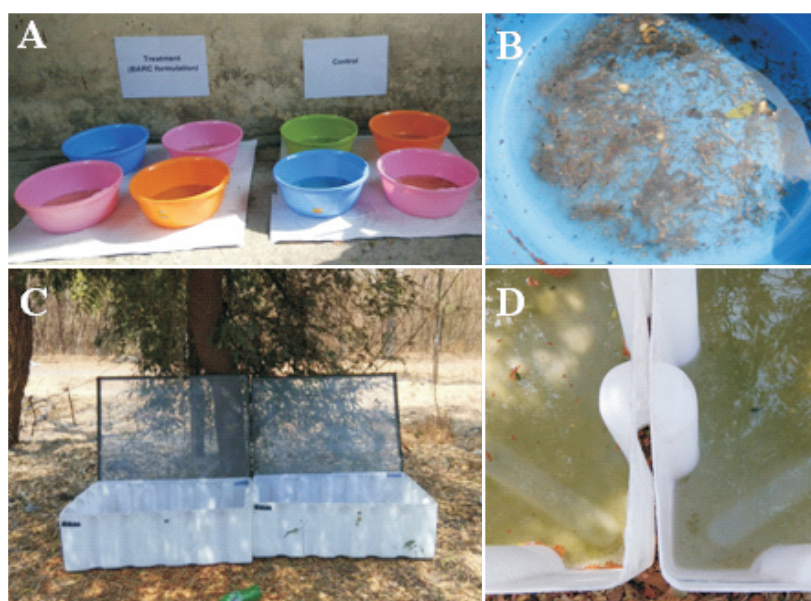


Fig. 4: Small-scale field evaluation of biopesticide formulation based on *Bacillus thuringiensis* subsp. *israelensis* strain ISPC-12. A. Plastic tub experiments (5 L cap.); B. Dead mosquito larvae due to *Bti* ISPC-12 biopesticide; C: Water tank with metallic mesh lid (200 L cap.) experiment; D: Dead mosquito larvae due to *Bti* ISPC-12 biopesticide (left) and live mosquito larvae in control (right) after 24 h.

experiments (Fig. 4B), respectively. Similarly, around 99% mortality was also observed in both *Aedes* and *Culex* mosquito larvae in water tank experiments (Fig. 4D). This suggests that *Bti* ISPC-12 has potential to use as biocontrol agent for mosquito control in field conditions.

Field studies

Field experiments were conducted in townships of Anushaktinagar, Mumbai and Raja Ramanna Centre for Advanced Technology (RRCAT), Indore. In both townships, mosquito breeding sites particularly drainages,

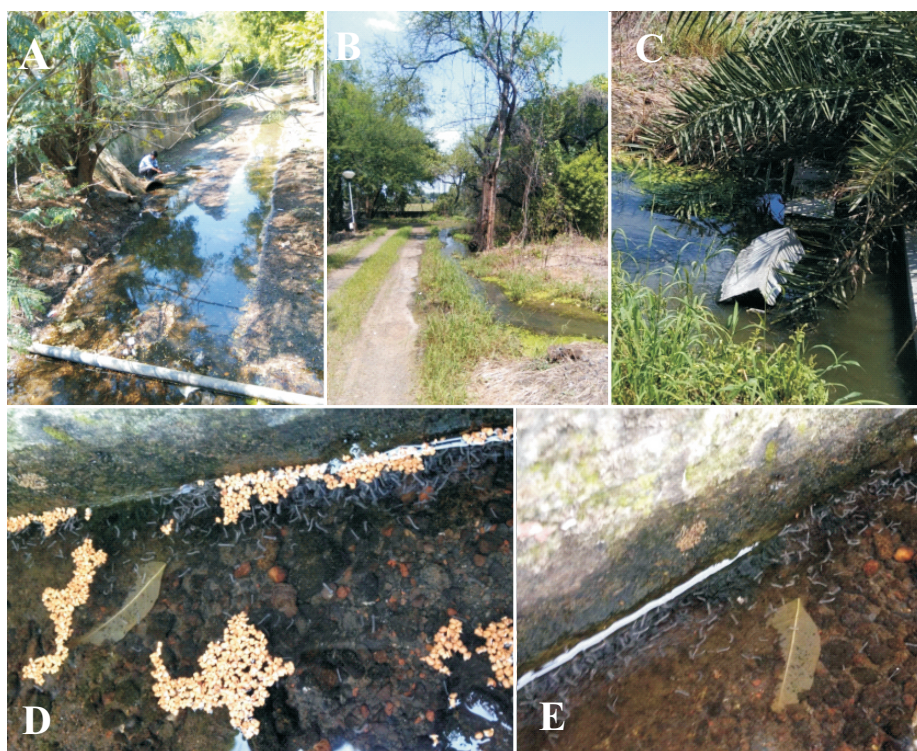


Fig. 5: Controlled field evaluation of biopesticide formulation based on *Bacillus thuringiensis* subsp. *israelensis* strain ISPC-12. Mosquito breeding sites at Anushaktinagar township, Mumbai (A) and RRCAT Indore township (B & C), Biopesticide application (D) and Post-application efficacy (E).

natural and sewage water stagnation sites were identified. The size of mosquito breeding sites at Anushaktinagar were ranging from 4-16 m² with immature stages of *Aedes* (3 sites) or *Culex* (1 site) (Fig. 5A), while around 4-10 m² area was identified for *Culex* (5 sites) in RRCAT township (Fig. 5B & C). In each location, identified mosquito breeding sites were treated with *Bti* ISPC-12 formulation (treatment) and separate untreated mosquito breeding sites were also earmarked. Pre-count (0 h) and post-counts (after 24 h treatment) of larvae of *Ae. aegypti* and *C. quinquefasciatus* in both treated and untreated habitats was monitored. Percentage reduction in larval population in treated habitats was estimated using Mulla's formula [18]. The population of larvae *Ae. aegypti* and *C. quinquefasciatus* in test habitats have varied with townships and breeding sites. Mosquito larval populations were significantly

reduced in treated breeding sites as compared to untreated sites. In Anushaktinagar, 93% *C. quinquefasciatus* larval reduction was observed at Site 1 whereas 93-94% *Ae. aegypti* larval reduction was recorded in sites 2-4. In case of RRCAT township, *Bti* ISPC-12 based biopesticide applied at 5 different sites resulted in 95-98% *Culex* mosquito larval reduction. It has been observed that local environmental factors play an important role in efficacy of the biopesticide in field [19]. Our field study results indicate that the efficacy of *Bti* ISPC-12 biopesticide formulation is effective at different geographical locations like Mumbai and Indore. This suggests *Bti* ISPC-12 biopesticide formulation could be an ideal substitution to chemical insecticides and has potential to reduce the larval population of different genera of mosquitoes thereby significantly contributing to mosquito control.

Conclusions

Mosquitoes are nuisance and responsible for transmitting several vector borne diseases. As mosquitoes are developing resistance to chemical insecticides, use of biological control agents like *B. thuringiensis* subsp. *israelensis* to control mosquitoes has become inevitable. Locally isolated *Bti* ISPC-12 strain shows higher toxicity towards *Aedes*, *Anopheles* and *Culex* larvae as compare to other isolates. Currently, very few biopesticides for mosquito control are available in India and most of them are imported and costly. Hence biopesticide formulation has been developed using this strain. Our studies have found that *Bti* ISPC-12 is effective against all larval stages of mosquitoes, amenable to mass production and formulation at cheaper cost, safe to mammals and easy to apply in the field condition. Thus, *B. thuringiensis* subsp. *israelensis* ISPC-12 is a potential biopesticide candidate for the management of mosquitoes.

*Corresponding author

Dr. Ramesh S. Hire

Acknowledgements

We are grateful to Dr. V. P. Venugopalan, Ex-Director, Bio Science Group (BSG), Dr. S. K. Ghosh, Associate Director, BSG, BARC and Dr. P. Suprasanna ex-Head, NA&BTD for kind support and encouragement. We thank Mr. Ashwin Patil for help in field experiments at RRCAT, Indore.

References

1. Boyce R., Lenhart A., Kroeger A., Velayudhan R., Roberts B., Horstick O. "Bacillus thuringiensis israelensis (Bti) for the control of dengue vectors: systematic literature review". Trop. Med. Int. Health, 18, (2013): 564-577.
2. Hancock P. A., Wiebe A., Gleave

- K. A., Bhatt S., Cameron E., Trett A., Weetman D., Smith D. L., Hemingway J., Coleman M., Gething P. W., Moyes C. L. "Associated patterns of insecticide resistance in field populations of malaria vectors across Africa". *Proc Natl Acad Sci U S A*, 115, (2018): 5938–5943.
3. Goldberg L. J., Margalit J. "A bacterial spore demonstrating rapid larvicidal activity against *Anopheles sergentii*, *Uranotaenia unguiculata*, *Culex univittatus*, *Aedes aegypti* and *Culex pipiens*". *Mosq. News*, 37, (1977): 355-358.
 4. Lacey L. A. "Bacillus thuringiensis serovariety *israelensis* and *Bacillus sphaericus* for mosquito control". *J. Am. Mosq. Control Assoc*, 23, (2007): 133-163.
 5. Dambach P., Baernighausen T., Traoré I., Ouedraogo S., Sié A., Sauerborn R., Becker N., Louis V. R. "Reduction of malaria vector mosquitoes in a large-scale intervention trial in rural Burkina Faso using *Bti* based larval source management". *Malar J*, 18, (2019): 311.
 6. Crickmore N., Bone E. J., Williams J. A., Ellar D. J. "Contribution of the individual components of the δ -endotoxin crystal to the mosquitocidal activity of *Bacillus thuringiensis* subsp. *israelensis*". *FEMS Microbiol Lett*, 131, (1995): 249–254.
 7. Ben-Dov E. "*Bacillus thuringiensis* subsp. *israelensis* and its Dipteran-specific toxins". *Toxins*, 6, (2014): 1222-1243.
 8. Lacey L. A., Mulla M. S. "Safety of *Bacillus thuringiensis* (H-14) and *Bacillus sphaericus* to non-target organisms in the aquatic environment". In Laird M., Lacey L. A., Davidson E. W. (ed.), *Safety of Microbial Insecticides*, CRC Press, 1990.
 9. WHO. "Microbial pest control agent: *Bacillus thuringiensis*; environmental health criteria". (1999): 217.
 10. Charles J. F., Nielsen-LeRoux C. "Mosquitocidal bacterial toxins: diversity, mode of action and resistance phenomena". *Mem Inst Oswaldo Cruz*, 95, (2000): 201-6.
 11. Rao A. S., Mahajan S. K. "Instability of mosquito larvicidal activity of *Bacillus sphaericus* (ISPC-6 = WHO-2377)". *Biotechnol Lett*, 12, (1990): 7–10.
 12. Hire R. S., Hadapad A. B., Vijayalakshmi N., Dongre T. K. "Characterization of highly toxic indigenous strains of mosquitocidal organism *Bacillus sphaericus*". *FEMS Microbiol Lett*, 305, (2010): 155-161.
 13. Hadapad A. B., Vijayalakshmi N., Hire R. S., Dongre T. K. Effect of ultraviolet radiation on spore viability and mosquitocidal activity of an indigenous *Bacillus sphaericus* Neide strain, ISPC-8. *Acta Tropica*, 107, (2008): 113-116.
 14. Tan S., Kern R. C., Selleck W. "The pST44 polycistronic expression system for producing protein complexes in *Escherichia coli*". *Protein Expr Purif*, 40, (2005): 385-395.
 15. Hadapad A. B., Hire R. S., Vijayalakshmi N., Dongre T. K. "Sustained-release biopolymer based formulations for *Bacillus sphaericus* Neide ISPC-8". *J Pest Sci*, 84, (2011): 249-255.
 16. WHO. "Guidelines for laboratory and field testing of mosquito larvicides issued by World Health Organization, Communicable Disease Control, Prevention and Eradication, WHO pesticide and evaluation scheme". WHO/CDS/WHOPES/GCDPP/2005.13.
 17. Abbott W. S. "A method of computing the effectiveness of an insecticide". *J Econ Entomol*, 18, (1925): 265–267.
 18. Mulla M. S. et al. "Control of chironomid midges in recreational lakes". *J Econ Entomol*, 64, (1971): 301–307.
 19. Zogo B., Koffi A. A., Alou L.P.A., Fournet F., Dahounto A., Dabire R. K., Baba-Moussa L., Moiroux N., Pennetier C. "Identification and characterization of *Anopheles* spp. breeding habitats in the Korhogo area in northern Côte d'Ivoire: a study prior to a *Bti*-based larviciding intervention". *Parasite Vector*, 12, (2019): 146.

0.1"

Nobel Prize 2020 in Physics

The orbits of stars within the central 1.0×1.0 arcseconds of our Galaxy. Note that the star S0-2 completes its orbit during the observation time. Other stars passed through at least one turning point of their orbits.

- S0-2
- S0-38
- S0-1
- S0-3
- S0-5
- S0-8
- S0-16
- S0-17
- S0-20
- S0-102

Keck/UCLA
Galactic Center Group

1995-2016

Courtesy: <http://www.astro.ucla.edu/~ghezgroup/blackhole.html>

On October 5th, 2020, Royal Swedish Academy of Sciences declared that the Nobel Prize in Physics would be awarded to Sir Roger Penrose of University of Oxford, Prof Reinhard Genzel of Max Planck Institute of Extraterrestrial Physics and Prof Andrea Ghez of University of California Los Angeles for their theoretical and observational work on black holes. In the prize motivation the Academy mentioned that Roger Penrose, in 1965, theoretically showed that *black hole formation is a robust prediction of general theory of relativity* [1]. Reinhard Genzel and

Andrea Ghez made *groundbreaking observations of stars orbiting the Milky Way's center that suggested that a supermassive compact object resides there* [1].

The idea of black hole fascinated people from different faculties starting from the professional physicists to the common people. Black hole forms because gravitational force affect light. Any gravitating object attracts light. If the gravitational force due to some object is so strong that light can not escape then black hole forms. Mathematically this concept is connected to the existence of space-

time singularities and formation of trapped surface, known as *event horizon*, within the framework of general theory of relativity. The first hint of such possibility came when Karl Schwarzschild, in 1916, solved Einstein's equation for a spherical mass M that does not spin. With his elegant and beautiful calculations Schwarzschild obtained the space-time metric around the mass and found that some terms in his solutions either vanish or diverge at $r=0$ and $r=2GM/c^2$ (known as Schwarzschild radius) giving rise to singularities in space-time. As Schwarzschild was ill, he sent his results to Einstein who presented

those results at the meeting of Prussian Academy of Sciences on 13 January 1916. Even though Einstein was fully aware of the work of Schwarzschild, he was not comfortable with those results. In 1939, Einstein wrote a paper in *Annals of Mathematics* [2]. In the last paragraph of the article Einstein wrote, *“The essential result of this investigation is a clear understanding as to why the ‘Schwarzschild singularities’ do not exist in physical reality.... The ‘Schwarzschild singularity’ does not appear for the reason that matter can not be concentrated arbitrarily. And this is due to the fact that otherwise the constituting particles would reach the velocity of light [2].”* However during 1930s astrophysicists were busy in resolving one important issue related to the stellar evolution. In 1931, Subramanian Chandrasekhar showed that the low to medium mass stars like Sun will end their life as white dwarf where the system is supported by electron degeneracy pressure against further gravitational collapse. The maximum mass of the white dwarf will be 1.4 times the mass of the sun, known as Chandrasekhar limit [3]. In 1939, J. R. Oppenheimer and G. M. Volkoff, using the general theory of relativity, found that stars in the mass range (0.7 - 3) times the solar mass will end their life as neutron star where the star is supported by neutron

degeneracy pressure against further gravitational collapse [4]. Therefore, astrophysicists asked what would happen to a star which has mass, say 50 solar mass? Oppenheimer and his student Hartland Snyder gave an answer using general theory of relativity [5]. They concluded for a sufficiently massive spherically symmetric star: *When all the thermonuclear sources of energy are exhausted, a sufficiently heavy star will collapse ... the radius of the star approaches asymptotically its gravitational radius; light from the star is progressively reddened, and can escape over a progressively narrower range of angles ... The total time of collapse for an observer co-moving with the stellar matter is finite... [5].* Somehow this work did not get much attention. Also a group of astrophysicists were skeptical about the final conclusion of the paper. It was thought that it could be due to the assumption of spherical symmetry. Therefore, the question of gravitation collapse, its connection to the space-time singularity and trapped surface remained unanswered. Oppenheimer joined Manhattan project and, later became the director of Institute of Advanced Study, Princeton, but never went back to research in gravitational collapse.

After a gap of almost twenty years, research on gravitational collapse started again with the discovery of quasars, pulsars and compact x-ray sources. In 1960, Roy Kerr, a mathematician from New Zealand, discovered an exact solution of Einstein's equations for a rotating massive object and determined the metric for the space-time around the rotating mass [6]. This is known as Kerr metric which describes the space-time around a rotating black hole.

In the same year Roger Penrose, a mathematician and philosopher of science, introduced a new approach, known as spinor approach to general relativity. It was actually a topological approach to describe the spacetime. At that time this was completely new to the relativists. Along with that he started describing the space-time associated with some phenomena



Roger Penrose

Indian connection to Roger Penrose's spinor approach to general relativity

In his observations on gravitational collapse without assumptions of symmetry, Roger Penrose concluded that deviation from spherical symmetry cannot prevent space-time singularities from arising, and in the process he challenged the applicability of the existing laws of Physics. Later, in 1970, working jointly with Stephen Hawking, he gave black hole formalism a strong basis with a mathematical theory that had a consequential effect in big bang cosmology. Here, the very basis of the work of Penrose was Raychaudhuri equation. Raychaudhuri equation was discovered by Amal Kumar Raychaudhuri, a professor at Presidency College, Calcutta (now Kolkata) in 1955 just one month after the death of Einstein. In his paper, *“Relativistic cosmology I”* published in *Physical Review*, Raychaudhuri showed that the space-time singularities are inevitable in general theory of relativity. In fact this very paper formed the basis of the work of Stephen Hawking as well.



Reinhard Genzel

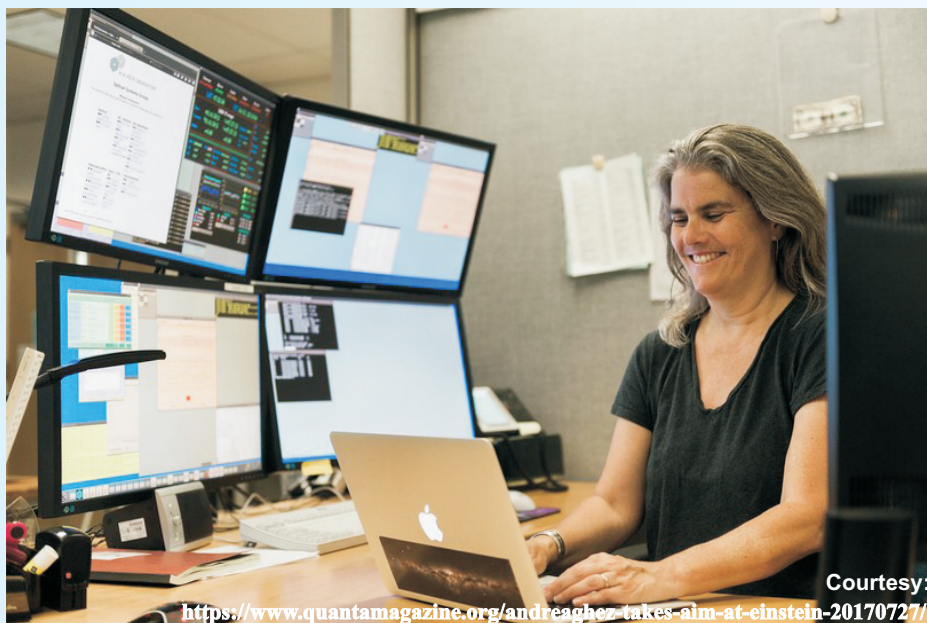
graphically which is known as Penrose diagram. With his new formalism Penrose investigated the possible formation of space-time singularity in gravitational collapse. In his paper titled, “Gravitational collapse and space-time singularities” published in *Physical Review Letters* in 1965 Penrose discussed gravitational collapse without assumptions of symmetry [7]. He concluded: “*deviation from spherical symmetry can not prevent space-time singularities from arising [7].*” Physically space-time singularity means a region in which space and time have become so locally distorted that present laws of physics are no longer applicable. The work of

Penrose had many important consequences. Later, in 1970, Penrose and Hawking proved a theorem which gave the mathematical theory of black hole formalism a strong basis. His work also has far reaching consequences in big bang cosmology. At this point it is important to mention that the very basis of the work of Penrose was *Raychaudhuri equation*. Raychaudhuri equation was discovered by Amal Kumar Raychaudhuri, a professor at Presidency College, Calcutta (now Kolkata) in 1955 just one month after the death of Einstein. In his paper, “Relativistic cosmology I” published in *Physical Review*, Raychaudhuri showed that the space-time

singularities are inevitable in general theory of relativity [8]. In fact this paper formed the basis of the work Stephen Hawking as well.

Once Penrose theoretically confirmed the existence of black holes the next question naturally arises how to detect them. As light can not escape a black hole, we can not see a black hole through astronomical observation directly. But the presence of a black hole can be sensed by observing its influence on the environment of the region where it resides. This idea led to the detailed observational study of active galactic nuclei (AGN) which were discovered by the radio astronomers in early fifties. AGN are distant galaxies with their centres more luminous ($\sim 10^{46-48}$ ergs/s) than the rest of the galaxy. The total luminosity of a galaxy like Milky Way is $\sim 10^{44}$ ergs/s. Astronomers argued that the such enormous amount of energy release is possible if there is a supermassive ($\sim 10^{7-9}$ times the mass of the sun) black hole at the center of the galaxy. As far as our own galaxy Milky Way is concerned, radio astronomers Bruce Balick and Robert Brown, in 1974, concluded that there is a bright compact supermassive object at the center of Milky Way and it is known as Sagittarius A*. Since then rigorous study was going on to find the exact nature of the object.

Reinhard Genzel and Andrea Ghez independently studied the motion of stars moving around the Sagittarius A*. The idea was to study the orbit and the periastron passage of a star. From such observations one can measure the mass and the compactness of Sagittarius A*. Andrea Ghez and her team studied the star S0-2 astrometrically (1995–2007) and spectroscopically (2000 – 2007) in the near-IR region using Keck 10m telescope in Hawaii while Reinhard Genzel and his team followed the same star over last 26 years using the Very Large Telescope (VLT) at



Andrea Ghez

European Southern Observatory (ESO), Chile. To study the orbits they introduced two new techniques—speckle imaging technique and adaptive optics. Using such techniques they could remove the blur in the image due to the turbulence in the Earth's atmosphere. Finally, in 2008, they reported that S0-2 has a period of 15.56 years (note that the Sun completes one revolution around Sagittarius A* in 200 million years!!), during its periastron passage it was just 120 AU away from Sagittarius A* and moved with a speed approximately 7650 km/s [9, 10]. From these observations they concluded that the mass of *Sagittarius A** is four million times the mass of the Sun and it is contained within a region

of size of our solar system. Therefore Sagittarius A is definitely a black hole.* Thus it took more than hundred years for the concept of black hole to get its final recognition which was a long due.

References

1. <https://www.nobelprize.org/prizes/physics/2020/summary/>
2. A. Einstein, *Annals of Mathematics*, 1939, 40, 922
3. S. Chandrasekhar, *Astrophysical Journal*, 1931, 74, 81
4. J. R. Oppenheimer and G. M. Volkoff, *Physical Review*, 1939, 55, 374
5. J. R. Oppenheimer and H. Snyder,

Physical Review, 1939, 56, 455

6. Roy P. Kerr, *Physical Review Letters*, 1963, 11, 237
7. R. Penrose, *Physical Review Letters*, 1965, 14, 57
8. A. Raychaudhuri, *Physical Review*, 1955, 98, 1123
9. R. Abuter et al, *Astronomy & Astrophysics*, 2018, 615, L15
10. A. M. Ghez et al, *Astrophysical Journal*, 2008, 689, 1044.

Compiled by
Dr. Subir Bhattacharyya,
 Astrophysical Sciences Division,
 BARC.

Solid State RF amplifiers developed in BARC power Superconducting Cavities in Fermilab



7 kW, 325 MHz Indian RF Power Amplifiers in Fermilab

State-of-art solid state radio frequency power amplifiers (RFPAs), designed and developed by BARC and productionized by ECIL, are now a part of Fermilab's beam facility in the USA. These were supplied between February and November 2020. Eight RFPAs are coupled to the single spoke resonator (SSR1) cavities of Proton Improvement Plan II (PIP II) Injector Test (PIP II IT) Facility in Fermilab. Earlier, at a nearly 100% transmission efficiency, H - beam operating from SSR1 clocked 7.5 million electron volts (MeV) energy. Recently 16 MeV beam energy was achieved. PIP II or High Intensity Superconducting Proton Accelerator (HISPA) of Fermilab entails upgrading its accelerator complex to deliver high intensity neutrino beams as well as to provide beams for a broad range of experiments, including the international Fermilab hosted Deep Underground Neutrino Experiment. Pursuant to the Science and Technology (S&T) Cooperation

agreement an implementing agreement was signed between Department of Atomic Energy, India and its US counterpart, Department of Energy (DOE). Further under Project Annex I to the Implementing agreement, India has agreed to make in-kind contributions in high intensity proton accelerator program of Fermilab. Radio Frequency Power is one among the sixteen technologies listed under Technical Cooperation under Project Annex I. The high power RFPAs are used to accelerate the beam through superconducting

cavities. The high efficiency RFPA systems reduce the wall-plug power consumption. Hence RFPA with best performance parameters is a critical technology and is a significant cost driver for superconducting accelerator operation. BARC had committed itself to design and deliver 09 units of 7 kW 325 MHz RFPAs for PIP II IT operations of Fermilab.

DAE envisages to set up HISPA either independently or jointly with DOE under the existing Indian Institutions and Fermilab Collaboration (IIFC). The 325 MHz RFPAs designed with stringent performance features such as high AC to RF efficiency, capacity to withstand high reflected power, high gain and phase stability, compliance to international EMI/EMC and environmental standards and low harmonics are critical to the performance of HISPAs both at Fermilab and DAE. A detailed technical article on this topic will follow in a forthcoming issue.

Article contributed by

Manjiri Pande, Gopal Joshi
(Accelerator Control Division, BARC, Trombay)



RFPA development teams of BARC and ECIL with the representatives of Fermilab

Largest radon calibration chamber in Asia-Pacific

Based on an innovative soil gas harvesting technique as a stable source of radon

Recently, two research papers in Scientific Reports, have been published detailing various aspects of radon calibration facility established at Centre for Advanced Research in Environmental Radioactivity (CARER), Mangalore under a DAE-BRNS collaborative project between Radiological Physics and Advisory Division, BARC and CARER.

This walk-in-type ^{222}Rn calibration chamber (volume of 22.7 m^3), with traceability to international standards, is the largest calibration chamber in the Asia-Pacific region. It adopts an innovative method for the generation of a wide range of ^{222}Rn concentrations (Bq m^{-3} to kBq m^{-3}) using natural soil gas as a continuous and steady radon source. It has a human-machine interface communication system, a programmable logic controller and sensor feedback circuit for control of environmental and radon parameters and data acquisition (Fig. 1).

This calibration facility will be useful for harmonising various radon measurement techniques and periodical calibration of several radon detectors being used across India for multiple applications that include (i) natural background radiation mapping, (ii) radon monitoring as earthquake precursor, (iii) radon emanometry for Uranium exploration, (iv) epidemiological investigations between residential radon and risk of lung cancer in public domain. A brief synopsis of the two published works is presented.

Part I: An innovative technique of harvesting soil gas as a highly efficient source of ^{222}Rn for calibration applications in a walk-in type chamber

This work describes the novel technique to harvest ^{222}Rn laden air



Asia's largest in-house developed radon calibration chamber installed at CARER under DAE-BRNS collaborative project

from soil gas of natural origin as a highly efficient source of ^{222}Rn for calibration applications in a walk-in type ^{222}Rn calibration chamber. It uses a soil probe of about 1m length to draw soil gas, through a dehumidifier and a delay volume, using an air pump. A new technique called "semi-dynamic mode of operation" in which, soil gas is injected into the calibration chamber at regular intervals to compensate for the loss of ^{222}Rn due to decay and leak, is presented. Harvesting soil gas as a calibration source has several advantages over the traditional methods of ^{222}Rn generation using finite sources (such as solid flow-through, powdered emanation, and liquid sources). They are:

- (i) Soil gas serves as an instantaneous natural source of ^{222}Rn , is convenient to use unlike the high strength ^{226}Ra sources, and has no radiation safety issues,
- (ii) It does not require licensing from the regulatory authority, and
- (iii) It serves as a continuous, non-depleting reservoir of ^{222}Rn , unlike

other finite sources.

The newly developed technique eliminates the need for expensive radioactive sources and thereby offers immense applications in research laboratories.

Part II: A periodic pumping technique of soil gas for ^{222}Rn stabilization in large calibration chambers: theoretical formulation and experimental validation

This work presents the mathematical formulation of a theory for determining the appropriate periodicity of pumping to get a good temporal stability with a universally acceptable deviation of 10% in the ^{222}Rn concentration. The model allows optimization of the pumping rate and duration and the injection periods (injection pump ON and OFF durations) for the semi-dynamic operation to achieve long term temporal stability in the ^{222}Rn concentration in the chamber. These computed pumping parameters are used to efficiently direct the injection of soil gas into the chamber. The

experimental validations in the calibration chamber (22.7 m³) are also presented. With this, the temporal stability of ²²²Rn concentration in the chamber was achieved within a deviation of 3% from the desired value.

References

Karunakara, N., Shetty, T., Sahoo, B. K. Kumara, K. S., Sapra, B. K., Mayya, Y. S. An innovative technique of harvesting soil gas as a highly efficient source of ²²²Rn for calibration applications in a walk-in type

chamber: part-1. Sci Rep 10, 1 6 5 4 7 (2 0 2 0) . <https://doi.org/10.1038/s41598-020-73320-9>.

Shetty, T., Mayya, Y.S., Kumara, K.S.,Sahoo, B.K., Sapra, B.K, Karunakara, N. A periodic pumping technique of soil gas for ²²²Rn stabilization in large calibration chambers: part 2-theoretical formulation and experimental validation. Sci Rep 10, 16548 (2020). <https://doi.org/10.1038>.

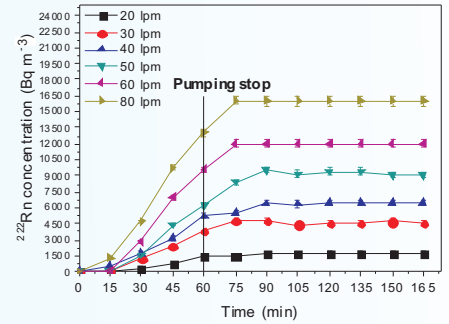


Fig. 2: Stability of Radon concentration in the calibration chamber for different pumping flow rates

Emission characteristics of ultrafine particles from bare and Al₂O₃ coated graphite for high temperature applications

Graphite is employed as structural material and fuel block in high temperature reactors (HTRs) due to its favourable properties at high temperatures. The performance of graphite at high temperature becomes a key input to the technology aiming towards its utilization in HTRs. An important issue of concern is the modifications in its structural characteristics due to postulated air ingress conditions, which needs to be addressed for ensuring safe operations. Under air ingress conditions, oxidation of graphite results in significant weight loss, usually above a threshold temperature termed as 'transition temperature'. Limited information is available defining the characteristics of aerosol particles generated above the transition temperature. The HTAF at IIT-BHU was commissioned to address such aerosol related issues. Fig.1 represents the experimental setup used in HTAF for studying the particle generation features in the

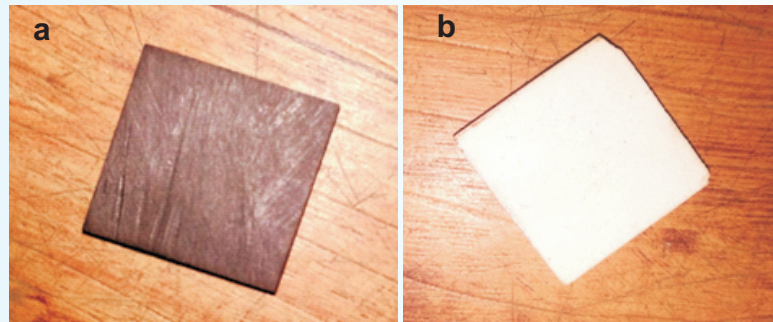


Fig. 1: Graphite samples (a) bare and b) coated with Alumina

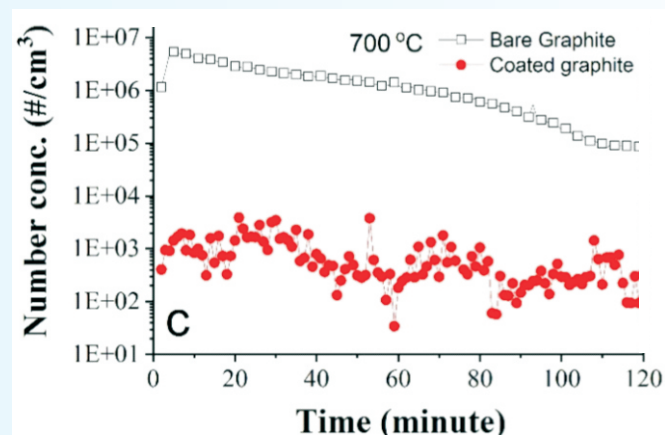


Fig. 2: Temporal evolution of Total particle number concentration at 700 °C

given context. In these experiments, transition temperature for high-density isotropic ultrafine grain graphite specimens (99.96 % carbon content by weight) was obtained as ~600 °C (Yadav et. al., 2019).

To avoid/delay the oxidation induced structural degradation, graphite is coated with an alumina (Al₂O₃) layer of thickness 100 μm. The present published article aims at studying the particle generation characteristics of both bare and alumina coated graphite specimen (Figure 2) exposed to high temperatures of 500°C, 600°C, 700°C, 800°C and 900°C. Results showed that, the particle emission followed a peaking pattern with the peak number concentration of $5.3 \times 10^6 \text{ cm}^{-3}$ at 700°C for the case of bare graphite (Figure 3). An important finding was that the coating was successful in preventing the particle generation. For instance, coated graphite at 700°C (100°C above the transition temperature) showed number concentration of particles about 3

orders lower than that for bare graphite.

To understand and interpret the oxidation induced particle emission characteristics of graphite at high temperature, simultaneous measurements of CO and CO₂ concentration profiles, the sample weight loss and scanning electron microscopic analysis were carried out. Generation of particles signifies the incomplete combustion of the specimen which is linked with the evolution profile of CO and CO₂ concentration. Coating layer suppressed the oxidation dynamics confirmed by the lesser frequency of pores, cracks and flakes for the residual specimens as seen in SEM images.

The analysis of the results of these experiments confirmed the shifting of transition temperature to a higher value for coated graphite. This signifies the increase in the safety margin of the operational constraints of HTRs in the worst case scenarios.

References

1. Yadav, S. K., P. Shukla, Manish Joshi, Arshad Khan, A. Kaushik, Ajit Kumar Jha, B. K. Sapra and R. S. Singh, Emission characteristics of ultrafine particles from bare and Al₂O₃ coated graphite for high temperature applications. *Sci Rep* 10, 14595 (2020). <https://doi.org/10.1038/s41598-020-71424-w>
2. Yadav, S. K., Manish Joshi, Y. Sharma, P. Shukla, A. Kaushik, B. K. Sapra, R. S. Singh, Physico-chemical characteristics of graphite aerosols generated during postulated air ingress accident. *Annals of Nuclear Energy*, 132, 100-107 (2019).

The research work discussed in the cited article was conceptualized by Radiological Physics and Advisory Division, BARC, and carried out in ‘High Temperature Aerosol Facility (HTAF)’ at IIT, BHU, developed with research funding from BRNS.

BARC Scientists Honoured



Dr. Kinshuk Dasgupta joined Materials Group of Bhabha Atomic Research Centre, Mumbai soon after graduating from 43rd batch of BARC Training School. He completed his Bachelors in Engineering (Metallurgy and Materials Science) from Jadavpur University, Kolkata, in 1999 and Ph.D

(Chemical Engg.) from the Institute of Chemical Technology, Mumbai. His PhD thesis received Ambuja Cement Best PhD Thesis Award. He visited University of Cincinnati, USA as a Fulbright Visiting Scholar during 2018-19. He received 'Young Metallurgist of the Year' in 2007 by Ministry of Steel Government of India, 'Young Engineer Award' in 2012 and 'Scientific and Technical Excellence Award' in 2017 by Department of Atomic Energy. Dr. Dasgupta has been awarded "Dr. N. J. Suchak Innovation Award 2019" by the Institute of Chemical Technology. Recently, "**Shanti Swarup Bhatnagar Prize 2020**" in **Engineering Sciences** has been conferred upon Dr. Dasgupta for his

work on carbon based nanomaterials and composites leading to the development of Bhabha Kavach, a light weight import substitute ballistic resistant jacket for Indian Armed Forces and Paramilitary Forces. Dr. Kinshuk Dasgupta has filed 2 Indian patents, has authored 3 book chapters, and has more than 90 publications in peer reviewed journals. In addition to Bhabha Kavach technology, he has transferred several technologies to the industries, including large-scale synthesis of carbon nanotubes and rare-earth magnetic alloy powder. Currently, he is serving as the Head, Advanced Carbon Materials Section, G&AMD, Materials Group, BARC and Associate Professor, Homi Bhabha National Institute, India.



Dr. A. K. Nayak is a mechanical engineering graduate from NIT Rourkela. He joined Reactor Design and Development Group in BARC in 1990 soon after completing one-year orientation course in nuclear engineering from 33rd batch of BARC Training School. In his career spanning across multiple decades, he made immense contributions on design aspects of Advanced Heavy Water Reactor (AHWR) and on

development of innovative passive safety systems of the reactor, which includes a novel methodology-APSRA- to address system reliability, state-of-the-art facilities for evaluation of AHWR design and vital safety aspects among others. For his unique expertise in reactor safety domain, Dr. Nayak is popularly known as "severe accident expert".

Some of his other major contributions include experiments with simulated molten corium in 700 MWe Indian PHWR calandria model for demonstrating the survivability of Pressurised Heavy Water Reactors during core meltdown accident, design of ex-vessel core catcher of AHWR and future IPWRs, demonstration of improved safety margins of water-cooled reactors under nano-fluids and analysis of associated flow instabilities, natural circulation flow and condensation-induced water hammering.

His developmental work on small and

modular reactors for addressing growing carbon emissions culminated into an innovative water-cooled 'Passive Safe Integral Reactor'. The special feature of these reactors is that they are fully manufactured and delivered at the project site for final installation. Dr. Nayak edited 3 books and published more than 350 papers in peer reviewed journals and conference proceedings. He is associate editor of Computational Thermal Sciences Journal and Frontiers in Energy Journal. He is a recipient of several awards, including Homi Bhabha Science and Technology Award, DAE Scientific Technical Excellence Award, DAE SRC Outstanding Investigator Award, DAE Group Achievement Awards, etc. **Recently, Dr. Nayak has been elected as a Fellow of INAE.** Besides, he is a Fellow of Maharashtra Academy of Science and JSPS RONPAKU Fellow. He is currently Outstanding Scientist and Head, Thermal Hydraulics Section, BARC and Professor, HBNI.



The Indian National Academy of Engineering (INAE) has elected **Dr. R. Balasubramaniam** (Control System Development Division) of BARC as a Fellow of National Academy of Engineering (FNAE) from 1st November, 2020 onwards.

The Fellowship recognises Dr. Balasubramaniam's contributions in the areas of Micro Nano Engineering, Diamond Turn Machining Technology and Technology Deployment for rural upliftment.

Dr. R.K. Bajpai of BARC Nuclear Recycle Group received Platinum Jubilee Lecture award of Indian Science Congress. The award recognises Dr. Bajpai's contributions in developing new technological solutions for safe disposal of radioactive wastes. Dr. Bajpai delivered the Platinum Jubilee Lecture on 'Technological Advances in the Back End of the Nuclear Fuel Cycle for Safe Geological Disposal of Nuclear Waste' at the Manipur edition of Indian Science Congress in 2018.

Dr. D. Bhattacharyya, Head, Synchrotron Science & Multilayer Physics Section of BARC Physics Group has been nominated to the committee of main editors of the popular *Journal of Synchrotron Radiation* published by the International Union of Crystallography (IUCr).

BARC Incubation Centre

Bhabha Atomic Research Centre launched a new capacity building programme to provide a boost to technology entrepreneurship in the country.

Under this initiative, young aspirants are encouraged to conceive new innovations from a range of BARC societal technologies at the newly launched Centre for Incubation of Technologies (BARCIT) in Mumbai.

Young innovators at BARCIT will avail technical consultancy and basic infrastructure facilities, including space, electricity, water, communication facility, etc. In addition, know-how in the form of

publications / BARC reports/technology documents/patent specifications, etc. readily available with BARC will be extended to them. The technology developed can then be licensed to the incubatee.

In the initial phase, BARC has lined up technologies in Food, Water, Electron Beam Welding, Medical equipments, Laboratory equipments, DAE Patents among others.

The announcement was made by Shri K. N. Vyas, Secretary Department of Atomic Energy and Chairman AEC on 31st October, 2020, coinciding with the 112th birth anniversary of legendary Dr. Homi Jehangir Bhabha,

BARC has lined up technologies in Food, Water, Electron Beam Welding, Medical equipments, Laboratory equipments and many others.

founder of atomic energy activities in India.

Bhabha Atomic Research Centre, Mumbai has a vibrant technology transfer and collaborative engagement in place with the private industry for faster deployment of societal technologies derived from nuclear energy R&D activities.

Training on radiological safety & regulatory measures for nuclear facilities

The 37th course on “Basic Radiological Safety and Regulatory Measures for Nuclear Facilities” was conducted by BARC Safety Council Secretariat (BSCS) at WIP, Kalpakkam during January 21-24, 2019. 65 participants from Kalpakkam Reprocessing Plant (KARP) and KARP II, and associated facilities, namely CWMF, WIP, WSCD, PRPD, AUGF and NDDP attended the course. Speakers at the event appreciated BSCS for coming out with the regulatory codes, guides and manuals specific to BARC facilities.

The training course was demonstrated through classroom lectures and interactive videos and covered all important topics such as

1. Regulatory framework of BARC
2. Radiation basics and natural radiation
3. Dosimetry and dose control
4. Radiation detection and measurement
5. Industrial, chemical and electrical safeties
6. Occupational health care
7. Preparedness and response for nuclear and radiological emergencies
8. Biological effects of radiation
9. Regulatory inspections
10. Event reporting and improvement of safety culture in the facilities

The training programme was well appreciated by all participants and dignitaries. As part of its work mandate, BSCS conducts many short-term training courses for the working personnel of BARC facilities.

Back Page Photo: Homi Jehangir Bhabha taking a stroll with Albert Einstein, Hideki Yukawa and John Wheeler c.1948 at the Institute for Advanced Study, Princeton.
(Photo by Wallace Litwin and Joseph Kringold)



Edited & Published by:
Scientific Information Resource Division
Bhabha Atomic Research Centre, Trombay, Mumbai 400 085, India
BARC Newsletter is also available at URL:<http://www.barc.gov.in>